Large-volume gravity flow deposits in the Central Carpathian Paleogene Basin (Orava region, Slovakia): evidence for hyperpycnal river discharge in deep-sea fans

DUŠAN STAREK[1], JÁN SOTÁK[2], JOZEF JABLONSKÝ[3] and RÓBERT MARSCHALKO[1]

[1]Geological Institute, Slovak Academy of Sciences, Dúbravská cesta 9, 842 28 Bratislava, Slovak Republic; dusan.starek@savba.sk
[2]Geological Institute, Slovak Academy of Sciences; Branch: Ďumbierska 1, 974 01 Banská Bystrica, Slovak Republic; sotak@savbb.sk
[3]Department of Geology and Paleontology, Faculty of Natural Sciences, Mlynská dolina 15, 842 15 Bratislava, Slovak Republic;
jozef.jablonsky@fns.uniba.sk

Abstract: The deep-water clastic systems of the Central Carpathian Paleogene Basin contain megabeds, which are developed in distinctive stratigraphic horizons and can be traced over long distances. These beds are characterized by great individual thickness (4–13 m), uniform lithology and internal structures. On the basis of their lithology, sedimentary structures and sequence development, the megabeds are characterized by 15 individual facies and interpreted from the viewpoint of flow hydrodynamics. The grain-size distribution and internal structures of the megabeds point to their deposition from uniform turbulent flows. The main controlling factor for generation of such large voluminous flows is inferred in the sea-level changes, when a relative rising of sea level during the Eocene/Oligocene boundary was responsible for long-lasting accumulation of the clastic supply at the basin margins. The large volume of detritus from river discharge and ravinement surfaces of flooded land was accumulated on the shore and in the conduit heads where the sediment was remobilized by other triggers. The flows generated by catastrophic floods during the early Rupelian sea-level lowstand are thought to be the most probably triggering mechanism. The large highly erosive hyperpycnal flows from flooding rivers could erode accumulated deposits in the conduit or on steeper basin-margin slopes and could cause progressive increase of the sand volume in the flow. Conduit flushing appears to be the most probable source of sediment for the very large voluminous flows that were responsible for deposition of the Orava megabeds.

Key words: Early Oligocene, Central Carpathians, megabeds, megaturbidites, hyperpycnal-flow deposits.

Introduction

Specific sedimentary units in the western part of the Central Carpathian Paleogene Basin (CCPB) are represented by "megabeds". They form a distinctive horizon of basin-fill formations with a great thickness (4–13 m), uniform lithology and finely structured sandstones and siltstones, which are developed in fining-upward beds. In the Orava region of the CCPB, the megabeds display a relatively broad lateral extent and distribution over a distance of 25 km (Fig. 1C). Moreover, similar occurrences of very thick sandstone beds from the identical stratigraphic level of other parts of the CCPB are recorded in the Podhale area (Kozinec beds *sensu* Golab 1959) and Spišská Magura area (Janočko & Jacko 2001; Soták et al. 2001; Sliva 2005).

Descriptions of megabeds, often referred as "megaturbidites" (e.g. Ricci Lucchi & Valmori 1980; Mutti et al. 1984; Bouma 1987; Labaume et al. 1987; Reeder et al. 2000; Remacha & Fernández 2003 and others), have been presented over the last decades in several studies. The megabeds with a great thickness and wide lateral extent, are considered to be a product of large-volume gravity flows (>2.5 km³ *sensu* Talling et al. 2007). They have been recognized mainly in acoustic and high-resolution seismic profiles (e.g. Piper et al. 1988; Rebesco et all. 2000; Reader et al. 2000; Anastasakis

& Pe-Piper 2006; Gee et al. 2006), drill cores (Reeder at al. 2000; Piper & Normark 2001) or in well exposed areas (e.g. Ricci Lucchi & Valmori 1980; Remacha & Fernández 2003; Talling et al. 2007; Muzzi Magalhaes & Tinterri 2010).

However, the deposition of a very thick bed by a single sedimentary event is relatively rare in deep-marine turbidite systems (Piper & Normark 2001). Furthermore the processes which can trigger voluminous turbidity currents able to influence depositional processes are still poorly understood and discussed (e.g. Piper & Normark 2009). The megabeds might be important as excellent markers for stratigraphic and seismic correlations over long distance, and useful in basin analyses (e.g. Doyle 1987; Pauley 1995; Remacha & Fernández 2003).

This study deals with the Orava megabeds in the Central Carpathian Paleogene Basin, with the aim of providing petrofacies, lithological and stratigraphical data and detailed descriptions of their sedimentary structures. These data enable us to recognize 15 individual facies characterizing the megabeds, with grain-size distribution, sequence organization and lateral transformation also reflecting the hydrodynamic conditions of their deposition. Our data in comparison with modern analogues of megaturbidites and other megabeds have been used for definition of the most probably model of large-volume flow initiation and deposition of megabeds in the western part of the CCPB.
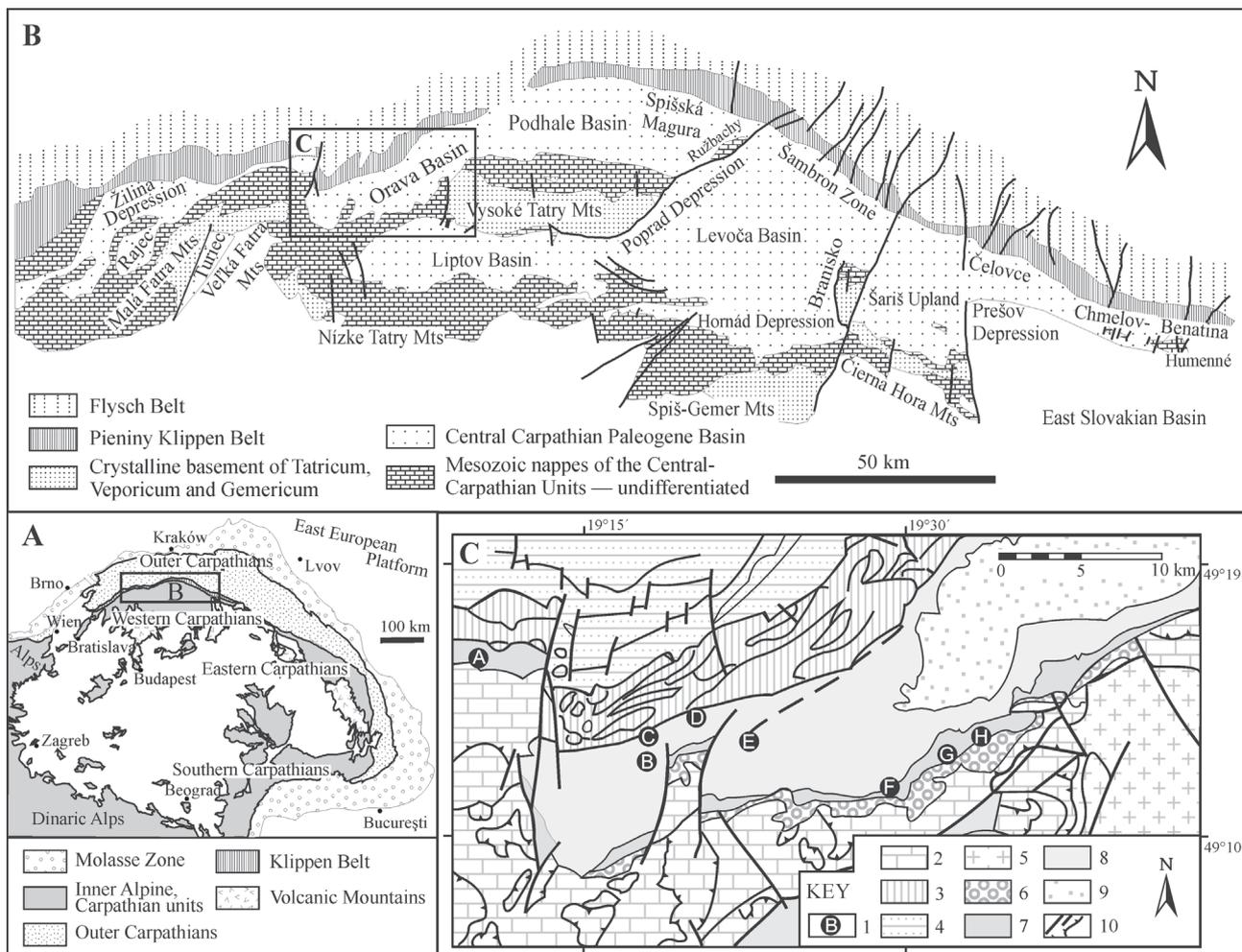
Fig. 1. A — Location of the study area within the Alpine-Carpathian orogen. **B** — The Central Carpathian Paleogene Basin system depicting structural sub-basins, basement massifs and surrounding units. **C** — Geological sketch of the Orava region (after Gross et al. 1993; Biely et al. 1996, modified) with situated megabeds studied. **Key: 1** — location of studied sections (A — Zázrivá (N49°15′11″, E19°10′29″); B, C, — localities near Dolný Kubín area (Veľký Bysterec — N49°12′24″, E19°17′05″, Záskalie locality — N49°12′51″, E19°17′30″); D — Kňažia (N49°13′55″,E19°19′45″); E — Pucov (N49°13′14″, E19°22′43″); F — Veľké Borové (Svorad plató section — N49°11′06″, E19°29′48″); G — Jobová Ráztoka (N49°12′10″, E19°32′1″); H — Huty (N49°12′27″, E19°32′56″); **2** — Mesozoic of the Inner Carpathians (undivided); **3** — Mesozoic of the Klippen Belt (undivided); **4** — Cretaceous and Paleogene of the Outer Carpathians (undivided); **5** — Magmatic rocks (Tatricum basement); the Central Carpathians Paleogene (**6** — Borové Formation; **7** — Huty Formation; **8** — Zuberec Formation; **9** — Biely Potok Formation); **10** — geological boundaries, faults and overthrust lines.

Background

Initiation processes for turbidity currents

Turbidity currents may be initiated by a wide range of processes at the edge of the continental shelf, which are connected generally with transformation of slumps, hyperpycnal flows from rivers, storm generated flows near the shelf edge, or combinations of these initiating processes (e.g. Normark & Piper 1991; Piper & Normark 2009). A very simplified description of these general processes is presented below.

Initiation by slope failure: The turbidity currents might be initiated by slope failures immediately in the seaward areas of a distributary mouth, where predominantly sandy sediments are accumulated. Such failures are particularly common in fan deltas (e.g. Hein & Syvitski 1992; Lrnne &

Nemec 2004; Carter et al. 2012). The form of sand failure depends on the efficiency of packing in the original sand body, which is a critical parameter for division of large bank failures into two types: liquefaction slope failures and breach failures (Van den Berg et al. 2002). Slump-generated turbidity currents show particular down-flow evolution. The sand and silt of the initial failures is essentially unlithified to form slumps and debris flows, which overcome sufficient distance and may be transformed through hydraulic jumps into turbidity currents on the steep slopes (e.g. Piper et al. 1999; Mohrig & Marr 2003).

Initiation by sediment-laden flows: Turbidites formed by direct freshwater sediment-laden flows are characteristic for steep and high-bedload rivers. These flows discharge on the narrow shelves, or prograde onto the basinal slopes to accumulate the fan deltas. Some sediments were deposited near

the mouth and subsequently reworked, but most hyperconcentrated coarse bedload would continue to flow seaward inertially (Prior & Bornhold 1989). Turbidity currents in fan deltas may often result from hyperpycnal flow (e.g. Mulder & Syvitski 1995; Mutti et al. 2000; Piper & Normark 2001; Mutti et al. 2003), although submarine landslides and remobilization of sediment are also widespread (e.g. Hein & Syvitski 1992; Carter et al. 2012).

Initiation by storms: These turbidity currents are initiated by storm resuspension of sediments near the shelf edge, mainly when the heads of the submarine canyons occur in the surf zone, from which they cross the narrow shelves. Suspension of sand and activation of seaward flows is considered to be the main initiation process of turbidites in canyon heads during storms (e.g. Fukushima et al. 1985; Prior et al. 1989; Mulder et al. 2001).

The multiple initiating processes: In submarine conduit heads and sandy deltas, multiple initiating processes for turbidity currents may interact in a complex manner. Erosion of deltafront channels or straight-sided prodeltaic channels by hyperpycnal flows can initiate failure and flushing of earlier deposited sands (e.g. Mitchell 2005).

Moreover, the deposition of sand during extreme floods is important on the prodelta, which then might fail due to depositional oversteepening (Milliman et al. 2007). Many hyperpycnal flows from rivers are predominantly muddy (e.g. Johnson et al. 2001), but may evolve into mixed flows by erosion of older sands from the conduit.

The initiating mechanisms and factors that trigger the deposition of large volumes and thicknesses of sediment in a single event are still a matter of discussion in literature. For example, the relationship between large-volume turbidity currents and sea-level changes is still poorly known. Several authors have suggested that a sea-level lowstand is a decisive factor for a non-steady stage, when terrigenous debris directly reaches the shelf margin, thus causing instability and susceptibility to sliding (e.g. Vail et al. 1977; Shanmugam & Moiola 1982, 1984; Reeder et al. 2000). Unstable environments can be influenced by different trigger mechanisms, which cause catastrophic collapse of the basin margin sediments and lead to the initiation of large-scale gravity flows. Similarly, when the sea level was at a maximum lowstand, Yose & Haller (1989) coupled the major collapse of outer ramps and upper slopes with the impingement of a storm wave base. The lowering of sea level resulted in progradation and cannibalization of the delta complex and a large amount of sand was transported by turbidity currents to the distal part of the basin (e.g. Postma 1995; Normark et al. 2006). On the contrary, Marjanac (1996) attributed the deposition of megabeds in the Eocene-Miocene flysch formations of the Central Dalmatia to the periods of accelerated sea-level rise, when the ground-water table rises, tides amplify, wave action increases, and the increasing pore-water pressure may provide favourable conditions for slope instability and collapse of the slope. Similarly, Ricci Lucchi (1990) reported great thicknesses of turbidites during highstand sea level. Rothwell et al. (2000) proposed that the generation of megaturbidites is more influenced by the rate of the sea-level changes than the amplitude of these changes.

Many authors regard seismic activity as a dominant trigger mechanism that causes upslope, large failures of the sediments. However, other important mechanisms (or their integration) that have also been suggested for triggering of large-volume gravitation flows and deposition of megabeds are connected with volcanic eruptions and earthquake activity (Anastasakis & Pe-Piper 2006; Anastakasis 2007), meteoric impacts (Iturralde-Vinent 1992; Dypvik & Jansa 2003), tsunami wave impacts (Cita et al. 1984; Cita et al. 1996; Heike 1984), the release of buried clathrates (Bugge et al. 1987), the over-supply and under-consolidation of sedimentary material (Doyle & Bourrouilh 1986), and also the stresses produced by tidal or river flow (Lowe 1976; Piper et al. 2007).

Geological setting

The CCPB lies inside the Western Carpathian Mountain Chain (Fig. 1A) and belongs to the basinal system of the Peri- and Paratethyan seas. The basin accommodated a forearc position on the destructive Alpine-Carpathian-Pannonian microplate margins and in the hinterland of the Outer Western Carpathian accretionary prism (Soták et al. 2001). The basin is mainly filled by turbidite-like deposits, which overlap the substrates of the pre-Senonian nappe units and their thickness reach up to a thousand meters. The age of the formations ranges from the Bartonian (e.g. Samuel & Fusán 1992; Gross et al. 1993) to the latest Oligocene (cf. Soták 1998; Olszewska & Wieczorek 1998; Gedl 2000; Soták et al. 2001, 2007) (Fig. 2). The sediments of the CCPB are preserved in many structural sub-basins, including the Žilina, Rajec, Turiec, Orava, Liptov, Podhale, Poprad, and Hornád Depressions (Fig. 1B). In the study area, the CCPB sediments are bounded by the Central Carpathian units in the south, while the northern boundary is represented by the Pieniny Klippen Belt (Fig. 1C), which represents a transpressional strike-slip shear zone related to a plate boundary (Csontos et al. 1992; Ratschbacher et al. 1993; Potfaj 1998).

The CCPB deposits are commonly divided into four formations (Gross et al. 1984; Fig. 2). The lowermost, Borové Formation consists of breccias, conglomerates, polymictic sandstones to siltstones, marlstones, organodetrital and organogenic limestones. These represent basal terrestrial and shallow-marine transgressive deposits (Marschalko 1970; Kulka 1985; Gross et al. 1993; Baráth & Kováč 1995; Filo & Siráňová 1996, 1998; Bartholdy et al. 1999). This formation is overlain by the Huty Formation, which mainly includes various mud-rich deep-marine deposits (e.g. Janočko & Jacko 1999; Soták et al. 2001; Starek et al. 2004). The overlying sediments of the Zuberec and Biely Potok Formations consist of rhythmically bedded and massive sandstones, which represent the various facies associations of sand-rich submarine fans (Soták 1998; Janočko et al. 1998; Starek et al. 2000; Starek 2001; Soták et al. 2001).

The megabeds of the Central Carpathian Paleogene Basin occur in the basal part of the Huty Formation and in the south-western and southern parts of the Orava region (therefore they are informally termed the "Orava megabeds"). Eight outctops were studied during field research (Figs. 1C and 3). The major outcrops occur near Dolný Kubín (Veľký
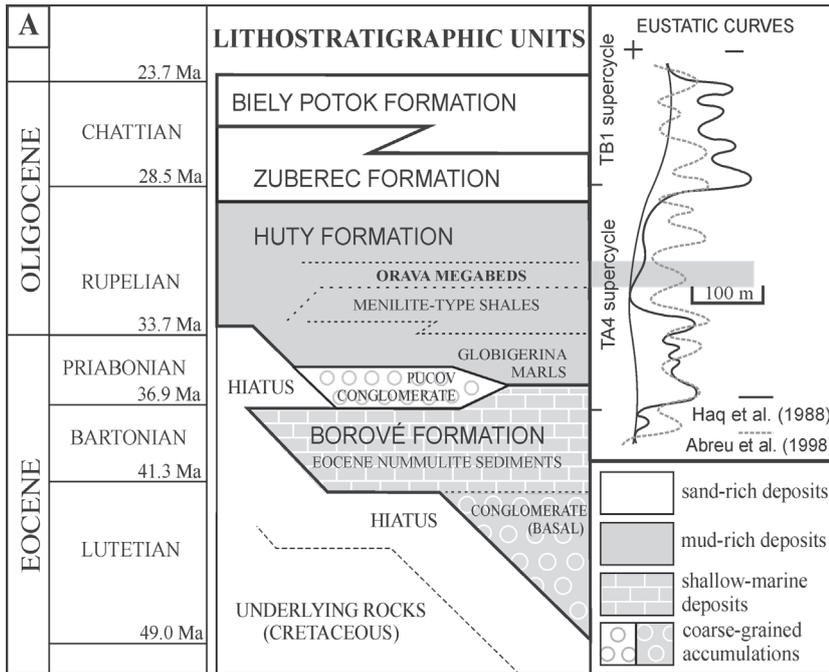
Fig. 2. Descriptive lithostratigraphy of the filling in the western part of the Central Carpathian Paleogene Basin. Nomenclature of the formations according to Gross et al. (1984, adapted). Biostratigraphy is based on the data from Olszewska & Wieczorek (1998), Starek et al. (2000), Starek (2001), and Soták et al. (2007).

Fig. 3. Representative logs of mudstone-dominant sedimentary facies with position of megabeds in the lowermost part of the Huty Formation. **B** — Veľký Bysterec; **C** — Záskalie (localites near Dolný Kubín); **D** — Kňažia; **E** — Pucov; **F** — Veľké Borové (Svorad plató);

G — Jóbova Ráztoka; **H** — Huty. For localization see Fig. 1C. **Key: 1** — conglomerates, sandstones and organodetrital limestones of the Borové Formation; **2** — conglomerates and breccias; **3** — megabeds; **4** — repetitively thin-bedded sequence; **5** — laminated limestones (Tylawa-type); **6** — brown, dark grey to black non-calcareous claystones (Menilite horizon); **7** — grey calcareous marls.

Bysterec and Záskalie locality), and in the bedrock of the Prosiek creek near Veľké Borové village (Svorad plató section). Additional megabeds occur near Pucov, Kňažia, Huty, Jobová Ráztoka and Zázrivá villages.

The megabeds appear in the lowermost part of the Huty Formation, where they developed from the menilite-type claystones directly above the pre-transgressive and transgressive sediments (e.g. in Svorad plató section on the northern slope of the Chočské vrchy Mts — Fig. 3F). The menilite interval is represented by non-calcareous, or weakly-calcareous dark mudstones that contain tuffite-bearing beds, biosiliceous horizons (cherts), breccia beds, and millimeter-scale intercalations of light carbonate-rich mudstones. This interval grades up to grey-calcareous claystones with siliciclastic megabeds (Fig. 4B). In another sections, the Globigerina marls and menilites of the Huty Formation are reduced, and the laminated sandstone megabeds directly overlie the Borové Formation (e.g. in Jóbova Ráztoka and Huty sections — Fig. 3G,H). Near Pucov (Fig. 3E) and Zázrivá villages, the megabeds occur within light calcareous claystones that overlie conglomerates, which are in some places over 100 m thick (Gross et al. 1982; Soták et al. 2007; Starek et al. 2012). The sections near Dolný Kubín (Fig. 3B,C) pass through mudstone-dominated sequences, which are intercalated by turbidite bed-sets, sandstone megabeds (Fig. 4A,C) and breccias.

The biostratigraphy and stratigraphic position of the Orava megabeds indicates that they belong to a distinct marker interval in the basal part of the Huty Formation, which spread over a great area of the basin. The megabeds show uniform thickness, usually at a distance of tens of meters within the outcrops. In spite of the possibility that these beds can have a great lateral continuity it is often impossible to correlate the megabeds to each
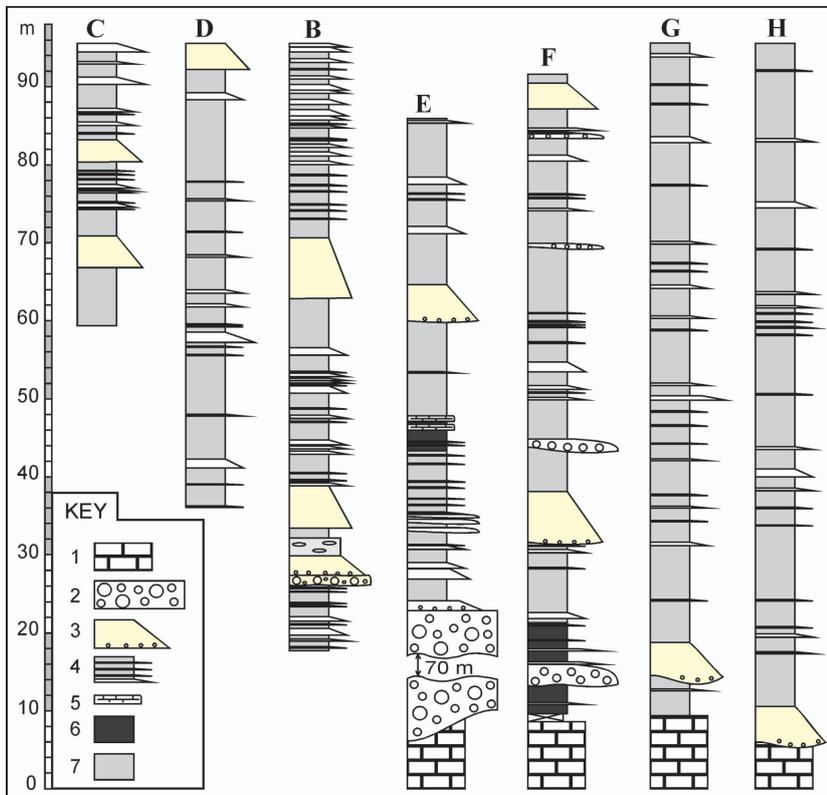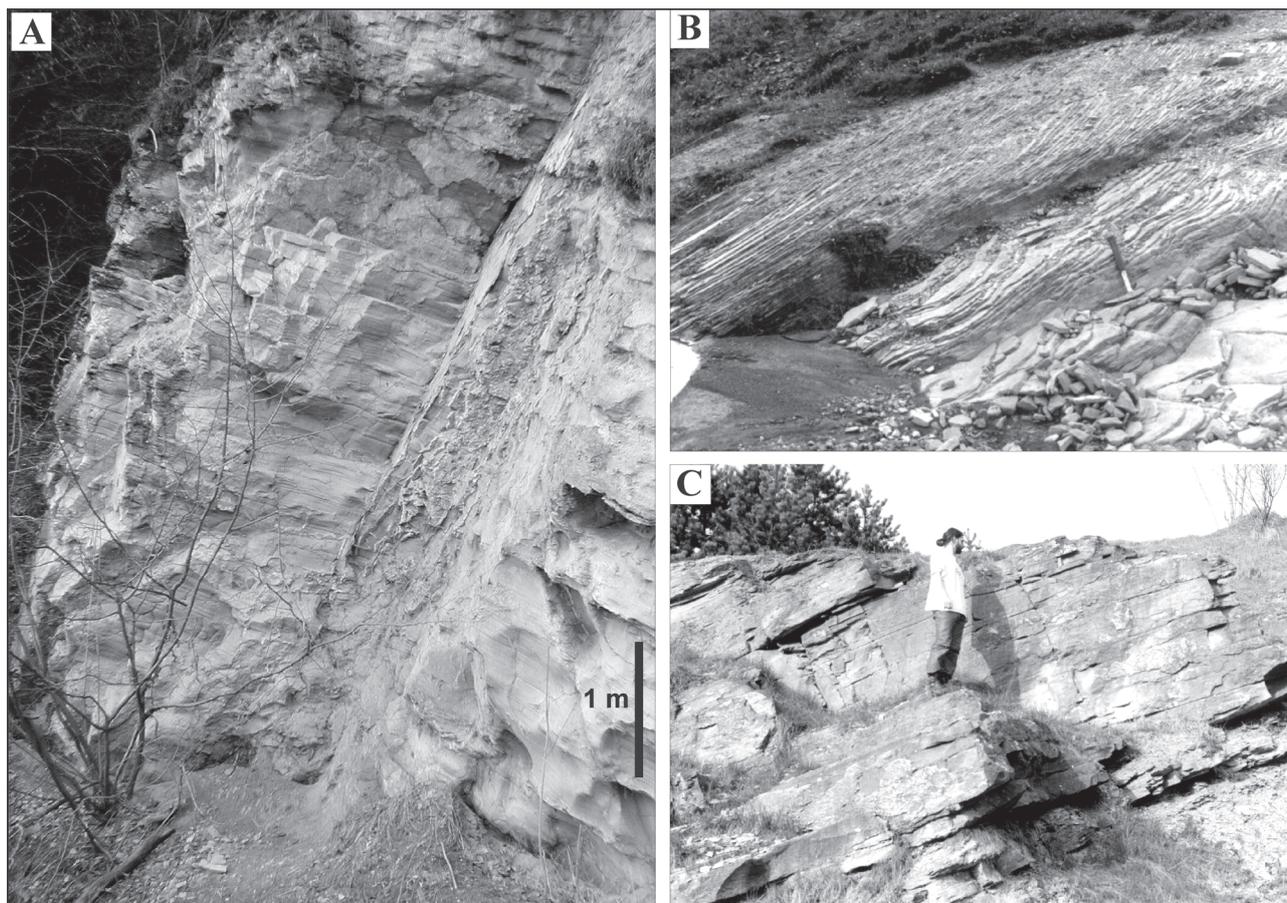
Fig. 4. Field exposures of megabeds. **A** — Finely structured part of the megabed at the Veľký Bysterec locality. Very thick laminated sandstones are dominant and they pass continuously to the siltstone in the uppermost part of the bed. **B** — Laminated sandstone part of up to 13 m thick megabed at Svorad plató (near Veľké Borové). **C** — Bed about 430 cm thick at Dolný Kubín locality.

other, because of the scattered nature of the key outcrops. The impossibility of correlation of individual beds over long distance, as well as poor knowledge about the paleotopography of the Central Carpathian Paleogene Basin due to post-Paleogene inversion, uplift and tectonic disintegration of the basin does not allow us to estimate the total volume of sediment transported during depositional events of individual megabeds. We can provide at this stage only very crude estimation of the minimum volume of individual megabeds in the Orava region of the CCPB which varies between 1.2 to 2.8 km^3.

Results

Sedimentary facies

The Orava megabeds are predominantly formed by sandstones and siltstones with varying grain size. They are developed in the form of fining-upward beds from a coarse-grained base to fine-grained sandstones, siltstones and gradually to claystones. One of the most important features of "megabeds" is their great thickness (Figs. 3, 4, 5), which is considerably greater than that of time-equivalent stratigraphic intervals in other parts of the depositional basin. The determination of the total thickness of the basal sandstone part of the megabeds was difficult due to a gradual transition into the overlying mudstones. We have defined the upper limit of the megabeds usually to the base of the overlying bed that markedly differs in grain size or to the base of occurrence of the light calcalerous hemipelagic mudstones. The bed thickness of this predominantly sandstone–siltstone–claystone sequence varies between 4–12 m near Dolný Kubín, and reaches up to 13 m near Veľké Borové and Huty.

The description and classification of the Orava megabeds is mainly based on descriptive parameters such as grain size, roundness, sorting, grain fabric, and sedimentary structures. In this analysis the grain-size and textural classification was done according to Blair & McPherson (1999). We used Powers (1953) standard index for shape classification of particles. The conglomerates are referred to as lithofacies C; the sandstones are referred to as lithofacies S, the siltstones as lithofacies Si, and mudstones as lithofacies M. Within the megabeds, 15 individual facies with their possible hydrodynamic interpretation were distinguished. Sedimentary facies have been depicted on the basis of the following hierarchical approach: (i) lithofacies based on lithology and (ii) subfacies distinguished on the basis of sedimentary structures.
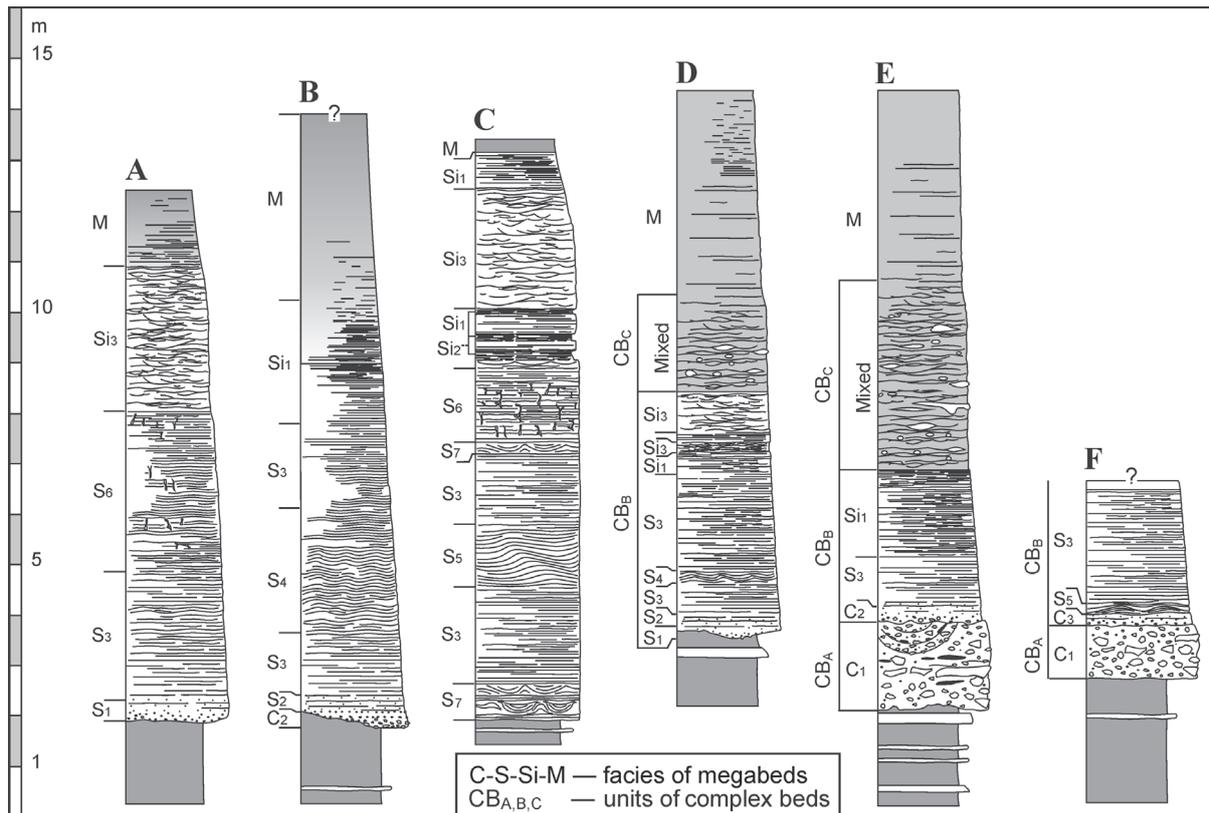
Fig. 5. Schematic log of megabeds. An explanatory text to the individual subfacies is given in the chapter "Sedimentary facies". **A, C** — Megaturbidites from Dolný Kubín localities. **B** — Megaturbidites from Svorad plató, Huty, Jóbova Ráztoka localities. **D, E** — Complex megabeds from Dolný Kubín localities. **F** — Complex megabed from Čremoš (Zázrivá).

C lithofacies: Conglomerate

C₁ subfacies: Massive, non-graded conglomerate

Description: Pebble to fine cobble, poorly sorted conglomerate which exhibits a disorganized texture (Fig. 6). They are compounded exclusively, or most prevailingly, by very angular to subangular clasts. The fabric varied widely from matrix- to clast-supported and generally, this subfacies has poorly sorted gravelly, sandy and muddy matrix (Fig. 6B). The conglomerate contains some "intraclasts" of dark non-calcareous claystones, which are irregularly scattered in a matrix-mixture of clay, silt and sand. Coherent, plastically deformed fragments of decimeter- to meter-scale blocks of sediments are a component of the C_1 subfacies (Figs. 6A, 11). The thickness of this facies varies between 110 and 180 cm.

Interpretation: The internal composition of coarse-grained C_1 subfacies and the presence of deformed blocks of sedimentary beds indicates deposition from dense flows with visco-plastic behaviour (non-Newtonian flows). Very similar facies are commonly referred to as debris-flow deposits or debrite (F2 facies *after* Mutti et al. 2003). This type of flow probably resulted from submarine landslide or multiple landslide phases (Gee et al. 2006), when large slabs of sediment could be detached, fragmented, and were capable of travelling enormous distances (Bugge et al. 1988; Masson et al. 1993). Erosion and disintegration of coherent blocks of sediment as well as erosion of the substrate during downslope movement would produce debris-flow matrix, which may enable the blocks to become buoyant and they can be rotated and plastically deformed during failure (Lastras et al. 2002; Gee et al. 2006).

C₂ subfacies: Unstructured ungraded to normally graded conglomerate

Description: Very poorly to poorly sorted, clast-supported, ungraded to normally graded, medium to coarse pebble conglomerate which can form a scoured unit (Fig. 11). This subfacies is characterized by angular to subrounded clasts. C_2 subfacies range in thickness from a few cm to 25 cm.

Interpretation: The basal parts of the megaturbidites, which are composed of a decimeter thick interval of the C_2 subfacies, can be described as R_3 sequence (*after* Lowe 1982) or F3 facies (*after* Mutti et al. 2003), which could represent a record of frictional freezing at the leading edge of gravelly dense flow.

C₃ subfacies: Unstructured to stratified inversely graded conglomerate

Description: Poorly sorted, clast-supported, inversely-graded, fine to coarse pebble conglomerate. This subfacies is characterized by angular to subrounded clasts. C_3 subfacies ranges in thickness from a few cm to about 20 cm.
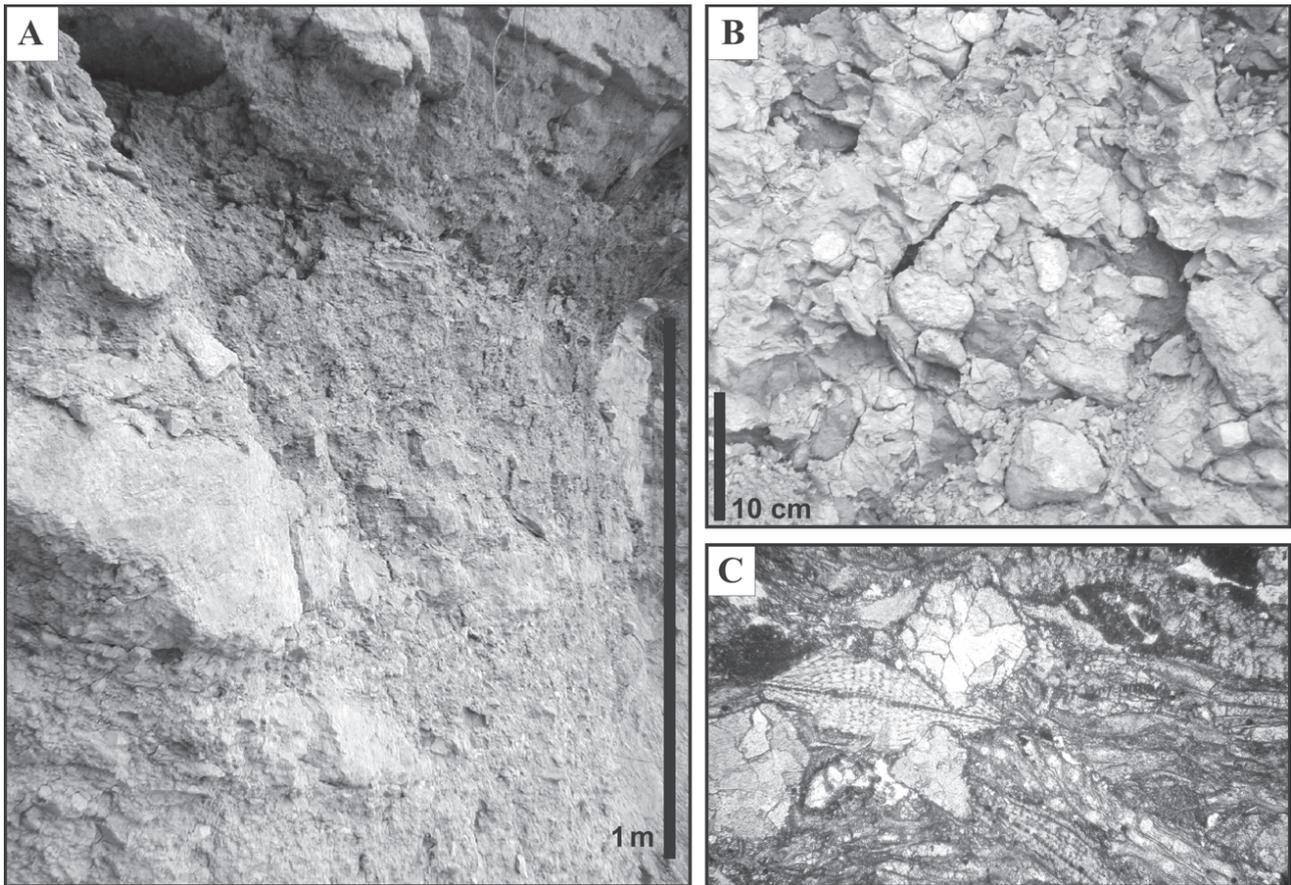
Fig. 6. A — Coarse-grained, poorly sorted, disorganized conglomerate with coherent fragments of older sedimentary rocks (C_1 subfacies) (Veľký Bysterec). **B** — Matrix- to clast-supported conglomerate with very angular to subangular clasts (detail view of C_1 subfacies). **C** — C lithofacies from outcrops near Dolný Kubín contain a large amount of biofragmental particles (detrital components of the Borové Fm). Enlargement 34×.
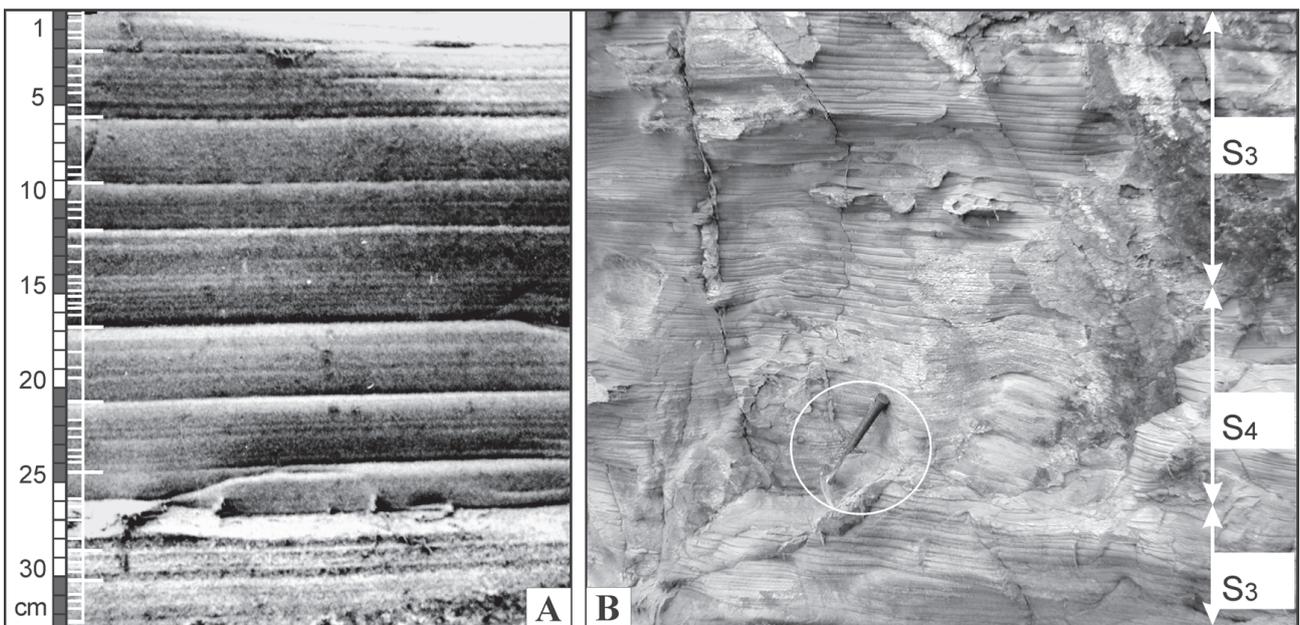

Fig. 7. Multiple intervals of a parallel lamination (Veľký Bysterec). **A** — The detail of parallel-laminated division (S_3 subfacies) with laminae ordered into "bands". **B** — In the middle of the S_3 subfacies, a division of "sinusoidal lamination" or "ripple laminae in phase" ca. 40 cm thick is developed (S_4 subfacies).

Interpretation: Grainflow or highly concentrated turbidity current. Equivalent to R_2 sequence (*after* Lowe 1982), which represents the deposits of gravelly high-density flows. Inverse grading is a result of deposition followed by a traction carpet stage. The C_3 as well as C_2 subfacies may be interpreted as the high-concentration flow observed at the base of many turbidity currents (Lowe 1982; Ghibaudo 1992; Mutti 1992).

S lithofacies: Sandstone

S_1 subfacies: Unstructured ungraded to normally graded coarse-grained sandstone

Description: Poorly sorted, usually ungraded, sometimes with normal grading, coarse-grained sandstones sometimes with dispersed granule to pebble-size clasts. S_1 subfacies ranges in thickness from a few cm to 40 cm.

Interpretation: A rapid accumulation of coarse-grained sands from dense sandy to gravelly turbidity current which bypass the zone of deposition of the preceding gravelly flows (S_3 flow type *after* Lowe 1982 or F5 facies *after* Mutti 1992).

S_2 subfacies: Stratified, inversely graded coarse-grained sandstone

Description: Poorly- to moderately sorted, crudely horizontally-stratified, pebbly/granule coarse-grained sandstones which form an interval up to 30 cm thick. Small pebbles and granules are angular to subrounded.

Interpretation: This subfacies indicates traction-carpet deposition (S_2 flow type *after* Lowe 1982). S_2 subfacies may be interpreted as the deposit of the dense sandy to gravelly flow (Ghibaudo 1992; Mutti 1992).

S_3 subfacies: Parallel-laminated medium- to fine-grained sandstone

Description: This subfacies is formed by a fining- and generally thinning-upward series of thin medium- to fine-grained sandstone laminae divided into discrete sets or "bands" (Fig. 7A). The thickness of these bands ranges from about 10 cm (at the base of the subfacies S_3) to 2 cm (at the top). Each sandstone bands consist of three to nine horizontal laminae with small thickness (0.3–1.3 cm) and relatively constant development. The laminae are inversely graded in the lower part and structureless in the upper portions. In some places, the laminae boundaries are highlighted by a concentration of pyrite, and locally also by accumulations of heavy minerals (predominantly zircon). Grain-size analysis of the sandstone laminites shows intervals of medium- to very fine-grained sand ($\phi1$–$\phi4$). The grains are angular and poorly sorted, and they have variable shapes. The S_3 subfacies ranges in thickness from a few decimeters up to 2 meters (Fig. 5).

Interpretation: The plane-parallel stratified sandstone could represent the deposit of a near-bed suspension generated by progressive turbulent mixing at the head of a sandy dense flow with relatively low rates of deceleration (Mutti et al. 2003). Each lamina can be considered to represent a traction carpet that is driven by basal shearing of an overlying turbulent flow. The cycle of "moving laminae" (i.e. bedwaves with small amplitude and long wavelength — *sensu* Best & Bridge 1992) was controlled by the growth and collapse of the traction carpets. The millimeter-thick (~1–2 mm) inversely graded divisions of the individual laminae, observed in parallel-laminated sands were apparently produced as energetic sweeps with fairly flat erosional surfaces, by the large turbulent eddies. In agreement with Hiscott (1994) we assume, that between local impingements caused by these isolated, more energetic sweeps, high rates of sediment fallout from suspension may have deposited the structureless, non-graded parts of sandy laminae.

S_4 subfacies: Sandstone with sinusoidal laminae in phase

Description: This is a relatively frequent subfacies within the studied megabeds. The ripple lamination in phase, as it was described by McKee (1939, 1965), is formed by two-dimensional bedforms which climb vertically. Bedforms have wavelengths between 0.3–0.8 m and their height varies from about 1 cm to
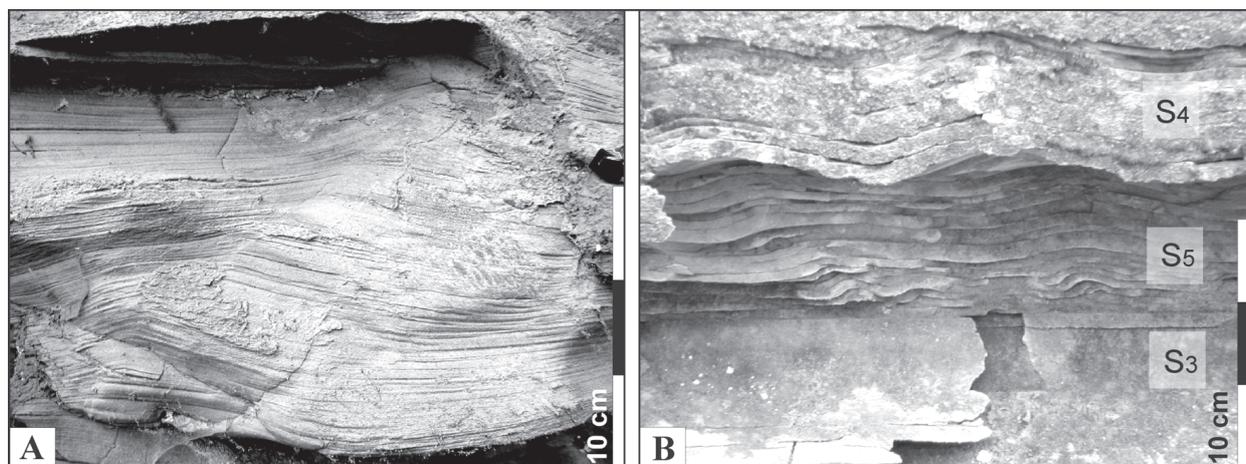

Fig. 8. The facies of "ripple" laminated sandstones at Veľký Bysterec locality (Dolný Kubín). **A** — "Ripple-drift cross lamination" (S_5 subfacies) characterized by its height angle of climb and by the complete preservation of bedforms. **B** — Vertical changes in lamination from parallel lamination (S_3 subfacies) to ripple-drift cross lamination (S_5 subfacies) and ripple laminae in phase (S_4 subfacies).

5 cm (Figs. 7B, 8B). The S_4 subfacies forms intervals a few decimeters up to more than 2 meters thick (Fig. 5B,D).

Interpretation: This type of sinusoidal ripple lamination consists of a series of ripples with symmetrical, sine-wave profiles and continuous laminae across the ripple system which is associated with a high rate of fallout of very fine cohesive sediments as shown by Jopling & Walker (1968).

S_5 subfacies: Sandstone with "ripple-drift cross lamination"

Description: "Ripple-drift cross lamination" (Jopling & Walker 1968) is type of climbing-ripples, which is characterized by a high angle of climb and by complete preservation of bedforms (Fig. 8A,B). The thickness of subfacies S_5 ranges from several decimeters to 1.2 m (Fig. 5C,F).

Interpretation: This is a typical traction plus fallout structure in which the interaction between rate of fallout and bedforms migration allows the formation of climbing sets of lee side laminae and the preservation of sandy stoss side laminae. The results are subvertical climbing ripples (Jopling & Walker 1968; Allen 1970).

S_6 subfacies: Laminated fine-grained sandstone with water escape structures

Description: This subfacies is almost identical to the S_3 subfacies of laminated sandstones but S_6 subfacies also includes common subvertical to vertical pillars or "pipes" that intersect lamination. Some laminae are moderately deformed around pipes.

Interpretation: The pillar structures represent fine water-escape conduits from which water and fluidized particles move upward, cutting and deforming overlying sediments (Owen 1987, 1996).

S_7 subfacies: Hydroplastically-deformed medium- to fine-grained sandstone

Description: Sandstone deformations vary from gentle to moderately strong upwardly-concave dish structures to convolute lamination (see Fig. 9).

Interpretation: Dish structure formation is connected with compaction and dewatering of unconsolidated sediments (Lowe & LoPiccolo 1974). The generating mechanism of convolute structures is linked to fluidization processes, which create gravitational instabilities (Owen 1996; Rossetti 1999; Neuwerth et al. 2006). The triggering mechanism of these structures is often related to processes of sediment gravity flows, overloading of sandstone beds, dewatering of unconsolidated sediments (e.g. Lowe & LoPiccolo 1974; Lowe 1975; Lowe & Guy 2000), or they should be induced by seismicity (Moretti et al. 1999; Neuwerth et al. 2006).

Si lithofacies: Siltstone

Si_1 subfacies: Laminated siltstone

Description: This subfacies is composed of coarse-grained to fine-grained laminated siltstone. The laminae of this subfacies are thinner, and finer than those of subfacies S_3. Si_1 subfacies forms an interval a few decimeters up to 2 meters thick (Fig. 5B,C,D,E).

Interpretation: The depositional mechanism of siltstone laminae is most likely the same as that in the laminated sandstones (S_3 subfacies) and reflects traction plus fallout processes associated with turbulent flows. The Si_1 subfacies can be considered equivalent to the Bouma T_d interval (Bouma 1962).
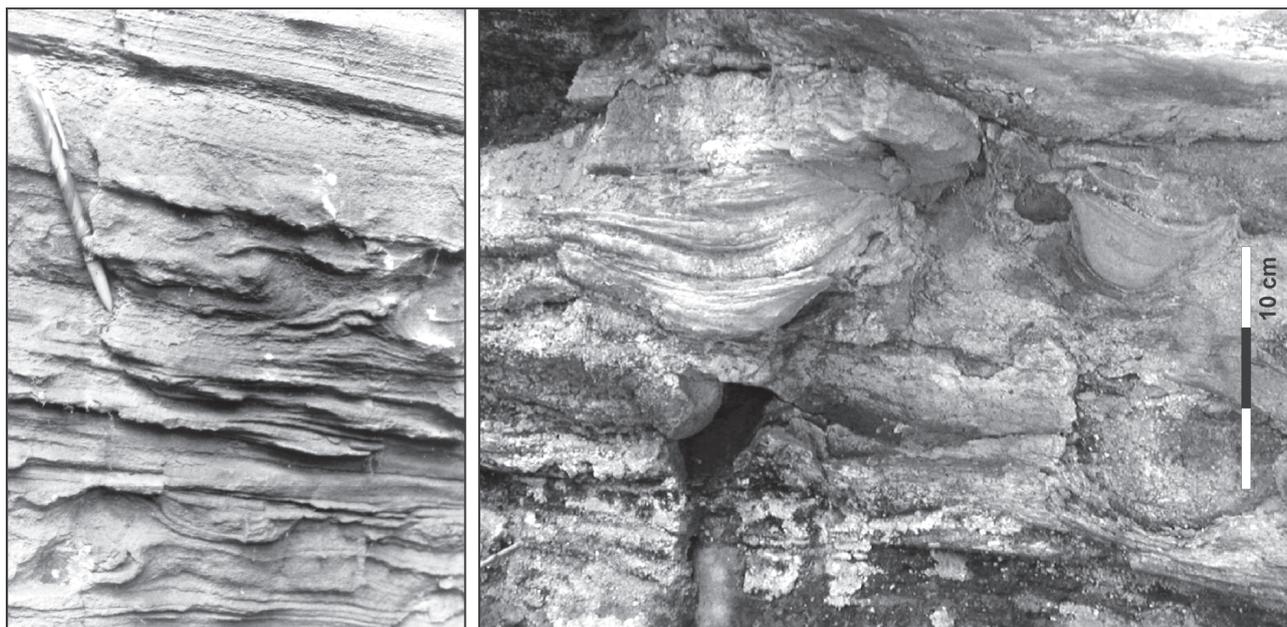

Fig. 9. Hydroplastically-deformed sandstones (S_7 subfacies).

Si₂ subfacies: Laminated muddy siltstone

Description: Coarse- to medium-grained siltstones with an increased clay content, which are characterized by fine, discontinuous wispy lamination. Si_2 subfacies forms intervals 10–20 cm thick (Fig. 5C).

Interpretation: Suspension fall-out during final deposition from a sediment gravity flow. The repetitive occurrence of muddy siltstones within clean laminated siltstones of Si_1 subfacies would be interpreted as a result of fluctuations in supply of sediment and speed of the flow.

Si₃ subfacies: Hydroplastically-deformed siltstone

Description: This subfacies is composed mainly of coarse-grained sandy siltstones with moderately to heavily deformed wispy lamination. Some deformations are similar to flat upwardly-concave dish-type structures which associate with vertical pillars. Although hydroplastic deformations are similar to those of subfacies S_6 and partly S_7, because of their occurrence in siltstone lithofacies we selected them as a single division.

Interpretation: The hydroplastic deformations within the Si_3 are probably associated with dewatering of unconsolidated sediments, when the suspended load settles too rapidly (e.g. Owen 1996; Lowe & Guy 2000).

M lithofacies: Massive dark mudstone

Description: This facies is composed of massive mudstones, having a $\phi > 8.0$. Although some parts reveal an increased content of silt (graded mudstones), the mudstones are mostly devoid of structure or grading. The M lithofacies shows the sedimentary characteristics of the Bouma turbidite division T_e or Stow division T_6 and T_7 (graded and ungraded turbidite muds respectively).

Interpretation: Suspension fall-out from static or slow-moving mud cloud. Final deposition from a sediment gravity flow event (e.g. Piper 1978).

Mixed lithofacies: Uniform mixture of sandy/silty claystones

Description: A unit up to 4 m thick with unimodal composition of sandy/silty claystones ($\phi 3.0–\phi 9.0$) is bounded by flat surfaces that represent primary bedding. Integral components of this bedding are formed by isolated, irregularly distributed eliptical pseudonodules of very fine-grained sandstones and siltstones (Fig. 10A,B). These pseudonodules are arranged with their long axes parallel to the bedding and range in size from a few cm up to a maximum of 40 cm. They are rounded in ellipsoidal and spiral shapes, and contain disrupted and intensely convoluted laminae (Fig. 10C). The central parts of the pseudonodules are highlighted by concentration of pyrite.

Interpretation: The unimodal grain-size composition (sandy/silty claystones matrix), thick and relatively large-sized body of the unit, its occurrence between undeformed strata, the presence of mostly rounded eliptical pseudonodules irregularly distributed within the unit, horizontal arrangement of pseudonodules and their deformed internal structures, as well as unrepeated occurrence of such a unit within the complex beds suggest that the Mixed lithofacies was not formed by normal sedimentary processes. We speculate that primarily deposited sediment with unconsolidated and semi-consolidated, siltstones and claystones as well as sporadic fine-grained sandstones, was affected by syn- to immediately post-depositional soft-sediment deformation. Soft-sediment deformation is often connected with liquefaction of sediment due to seismic shaking that lowered drastically its bulk density and shear strength allowing sinking and consecutive deformation of the overlying silty/sandy layers (Rodríguez-Pascua 2000; Davies et al. 2004). The formation of isolated or detached pseudono-
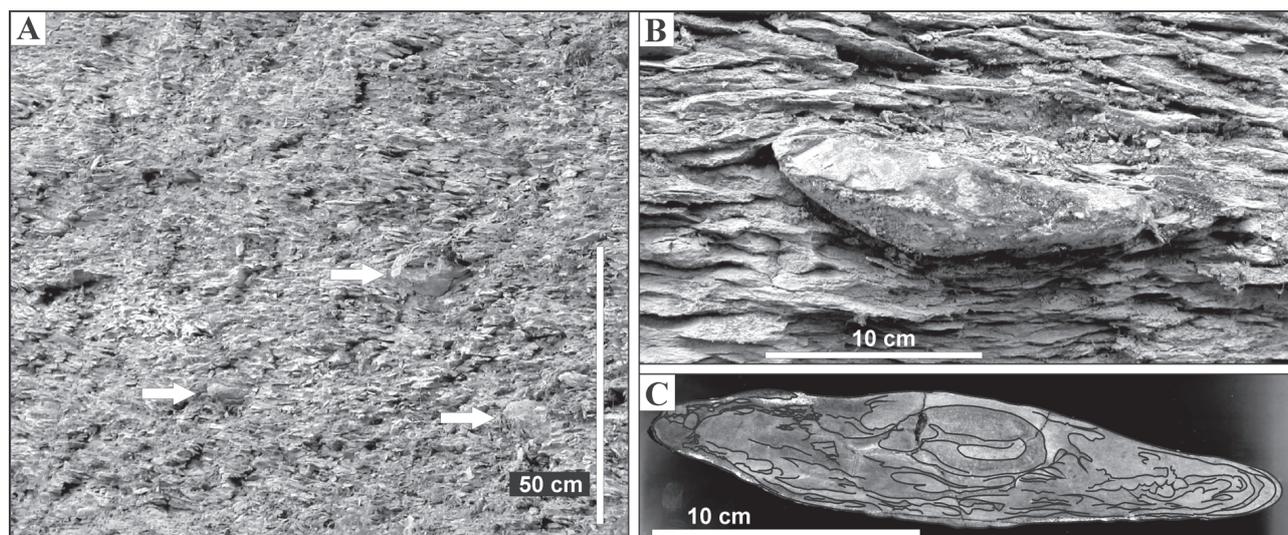

Fig. 10. A — A uniform mixture of sandy/silty claystones (Mixed lithofacies) with isolated elliptical pseudonodule of very fine-grained sandstone (Veľký Bysterec). **B** — A detailed view of the pseudonodule within sandy/silty claystones. **C** — An internal structure of many pseudonodules indicate plastic extruding and strong deformation of laminae.

dules resulted from the sinking of load casts in water-saturated fine-grained sediments (Kuenen 1958). The contorted laminae within the nodules (Fig. 10C) represent the original laminations of a silt and fine sand accumulation that was deformed as the beds underwent liquefaction and separation into a number of pseudonodular packets (Maurya et al. 1998; Davies et al. 2004).

However, similar division comprising a graded muddy sandstone/siltstone with a distinctive content of small pseudo-nodules and fragments of microfolded laminae is interpreted as syn-depositional deformation of primarily deposited thiner sandy, silty and muddy beds which resulted from multiple reflections of an upper turbulent suspension deposited from a large-volume flow (Remacha & Fernández 2003).

Facies association

Two types of megabeds were distinguished in the Orava region (Fig. 5). The first type is represented by thick separated beds, which have been classified here as "megaturbidites" (e.g. Svorad plató, Jóbova Ráztoka). Megaturbidites do not present internal erosive surfaces or amalgamation surfaces as well as grain size breaks (Fig. 5, logs A,B,C). An interesting aspect of the studied megaturbidites is the pure absence of thick, massive, structureless sandstone/siltstone parts within the beds. Nearly all lithofacies are finely structured. Each megaturbidite is a discrete bed, which recorded a single sedimentary event. The second type is represented by complex beds (CB) (e.g. Dolný Kubín, Čremoš; Fig. 5, logs D,E,F) that consist of the following successive units (from base to top): (1) coarse-grained, poorly sorted, disorganized breccia (CB_A); (2) the heterolithic unit equivalent to the megaturbidite (CB_B); (3) the deformed unit of the clayey siltstones (CB_C).

In general, the megaturbidite-type beds show a typically fining-upward trend in grain size from conglomerates and coarse-grained sandstones to fine-grained sandstones, siltstones and homogeneous mudstones. This trend reflects a gradual decrease in flow velocity and competence.

The lowermost parts of the megaturbidites are composed of relatively thin gradational intervals of C_2, C_3 and S_1 subfacies. The conglomerates of C_2 subfacies usually fill small-scale, shallow and laterally pinched-out scours. They can vertically and laterally pass into unstructured pebbly/granule sandstones of the S_1 subfacies. The S_1 subfacies is commonly developed directly at the base of megaturbidites (e.g. Záskalie, Kňažia and Veľký Bysterec sections), which have the flat base-bed surfaces with the sporadic occurrence of flute marks and tool marks. Inversely graded conglomerates of the C_3 subfacies are relatively rare. This subfacies is developed above the C_2 subfacies and usually vertically passes into the stratified, inversely graded S_2 subfacies. The S_2 subfacies forms an interval up to 35 cm thick in the uppermost parts of the gradational interval and upwards usually rapidly fine-down to medium-grained laminated sandstones of the S_3 subfacies. Multiple intervals of parallel lamination form the most evident internal structure of the sandstone part of these megabeds (Fig. 4). The S_3 subfacies can occur as an interval more than 2 m thick occasionally at the base of the megabeds (e.g. Kňažia, Záskalie), but more frequently it follows the S_1 and S_2

subfacies (e.g. Svorad, Pucov, Jóbova Ráztoka etc.). These parallel-laminated sandstones grade upward into laminated siltstones (Si_1 subfacies) and mudstones (M lithofacies). The sandstones with ripple lamination in phase (S_4 subfacies) are relatively common (e.g. Svorad locality) and the upper boundary of this subfacies is also gradual and usually again passes upward into fine-grained, parallel-laminated sandstones of the S_3 subfacies (Fig. 7B). A more uncommon type of structure in the megaturbidites is represented by the ripple-drift cross lamination (S_5 subfacies). This structure has been observed only in the Veľký Bysterec and Čremoš sections (Fig. 5, logs C and F), where the parallel lamination of the S_3 subfacies is locally associated with intervals of ripple-drift cross lamination. The transition of parallel lamination to ripple bedforms (S_{4-5} subfacies) might be caused by a temporal decrease in the fall-out velocity of the flows through intermediate increase in their shear velocity. The bed characterized by an alternation of different bedform types and subfacies may be interpreted as being deposited from unsteady, pulsating flows. The even and parallel-laminated siltstones (Si_1 subfacies) of the megaturbidites are usually developed as an interval a few decimeters up to 2 meters thick which records the transition between sandstones and claystones. This trend is typical of several megaturbidites at outcrops near Svorad plató, Huty, Kňažia and Jóbova Ráztoka (Fig. 5, log B; Fig. 4A,B). The upper parts of the megabeds are occasionally formed by 10–20 cm thick intervals of the laminated muddy siltstones (Si_2 subfacies). The uppermost parts of the megaturbidites are composed of mudstone lithofacies. The transition between the Si lithofacies and M lithofacies is gradual. The thickness of the dark turbidite mudstones varies from about 3 m (at Pucov and Svorad sections; Figs. 3E,F and 5B) to about 5 m (at Huty, Jóbova Ráztoka sections; Figs. 3H,G and 5B). However, because of the position of the megabeds within muddy deposits of the Huty Formation, the total thickness of mudstones belonging to the megaturbidites, cannot be correctly defined. The hemipelagic interval of lighter massive calcareous mudstones occurs locally above the M lithofacies (e.g. Huty, Jóbova Ráztoka, Svorad localites; Fig. 5, log B), but it was not possible to distinguish these two types of mudstones at localities near Dolný Kubín. The rapid deposition of the Orava megabeds is manifested by the presence of water escape structures (e.g. Lowe 1982; Lowe & Guy 2000), and other types of dewatering structures. Some megabeds near Dolný Kubín contain 20 up to 150 cm thick intervals of the S_6 subfacies, which are almost identical with the laminated S_3 subfacies (and often associate with this), but they also contain common subvertical to vertical streaks similar to the water-escape pillars. These pipe-like linear structures are either randomly distributed, or they exhibit a tendency to occur in the upper sandstone intervals of the megabeds. Hydroplastically-deformed sandstones of the S_7 subfacies form centimeter- to decimeter-thick intervals which show a limited lateral continuation from tenths of meters to a few meters, and they are surrounded by non-deformed laminated sets (S_3 subfacies). The S_7 subfacies is situated especially in the lower part of the beds and often occurs in megaturbidites near the Dolný Kubín–Veľký Bysterec locality (Fig. 5A,C,D). The coarse-grained siltstones with deformed wispy lamination, flat dishlike

structures and fine vertical water-escape conduits (Si$_3$ subfacies) form intervals that range in thickness from 30 cm to 3 m. The Si$_3$ subfacies predominantly develop on the upper parts of megabeds near the Dolný Kubín–Veľký Bysterec locality (Fig. 5A,C,D). Many intervals of siltstones lithofacies display transition from laminated siltstones (subfacies Si$_1$) to hydroplastically-deformed siltstones (subfacies Si$_3$).

The CB$_A$ unit of the complex beds, developed on the base of some composite megabeds (e.g. Veľký Bysterec and Čremoš sections), represents deposits from debris flows. This unit is characterized by relatively coarse-grained conglomerates with a disorganized texture and presence of deformed fragments and blocks of sediments (C$_1$ subfacies). The thickness of the CB$_A$ unit ranges from 110 cm to 180 cm (Figs. 5E,F and 11). The base of the conglomerates exhibits a slightly erosive character. The upper part of C$_1$ subfacies was furrowed by small-scale erosional scours which are developed at the base of clast supported conglomerates of the C$_2$ subfacies (Veľký Bysterec; Fig. 11). The furrows point to the erosion of the soft upper surfaces of debris-flow deposits by subsequent gravelly dense flows.

The CB$_B$ unit is composed of the facies, which in general are very close to those originally described within megaturbidites. The vertical arrangement of the subfacies of the CB$_B$ unit corresponds to the fining-upward grain-size trend of megabeds. The uniform mixture of sandy/silty claystones with pseudonodules (Mixed lithofacies) is well documented as the CB$_C$ unit in the Veľký Bysterec section (Figs. 5D,E and 10A), where they are developed above thick, laminated siltstones (Si$_1$ subfacies) or hydroplastically-deformed siltstones (Si$_3$ subfacies) of the CB$_B$ unit. The CB$_C$ unit is overlapped by thick massive mudstones (M lithofacies).

Lithology

A lithological analysis of the Orava megabeds highlights the differences in their petrographic composition in dependance on their grain-size composition. The coarse-grained conglomerates with a disorganized structure and angular clasts (C$_1$ subfacies) are composed almost exclusively of carbonate rocks from older Mesozoic and Paleogene units. The clast composition reflects the source areas formed by the Mesozoic basement units (Choč and Krížna Nappes) and Late Eocene to Early Oligocenne sedimentary units (detrital components of the Borové Formation, and intraclasts of dark non-calcareous claystones of the Huty Formation). The similar composition

with prevalence of the carbonate rocks has also been found in the C$_2$ and C$_3$ subfacies, in which a significant portion of detrital particles (up to 10 %) is composed of foraminiferal tests (mainly nummulites; Fig. 6C). The bioclasts are common mainly in the megabeds near Dolný Kubín and Pucov, but they are more rare in the gradational intervals of the megabeds at the others localites.

The content of quartz and siliciclastic components increases markedly over the carbonates in the upper intervals of the S$_1$ and S$_2$ subfacies, and these clasts became dominant in all sandstone and siltstone subfacies. The results of petrographic analysis show that the amount of quartz and stable rock grains reaches up to 47–52 % in the parallel-laminated sandstones (S$_3$ subfacies), and their proportion increases moderately from the base to the top of this subfacies. The content of unstable rock grains, which predominantly involve carbonates, is approximately 17–23 %. The remaining proportion of sediment is composed of a matrix and carbonate-fill cement from the intergranular pores. The medium- to fine-grained sandstone lithofacies and siltstone lithofacies often contain large amounts of coal particles to millimeter-thick coal seams and up to millimeter-sized flakes of mica.

Paleocurrent orientation

The studied megabeds basically lack paleocurrent indicators, or they are relatively poor in typical current indicators such as flute marks and current cross-bedding structures. In

Fig. 11. The complex beds (CB) (Veľký Bysterec). CB$_A$ unit characterized by coarse-grained, poorly sorted, disorganized conglomerate (C$_1$ subfacies) with plastically deformed, meter-scale blocks of sediments (white arrows). Take note of an indication of primary bedding preserved within the blocks of sediments. The upper part of C$_1$ subfacies was furrowed by small-scale erosional scours (black arrows), which points to the erosion of subsequent gravelly dense flows represented by clast supported conglomerates of C$_2$ subfacies at the base of the CB$_B$ unit.

most of the outcrops, the megabeds are surrounded by mudstones, siltstones and fine-grained thin sandstones with trace fossils on the flat bed surfaces. The exception to this occurs in area near Dolný Kubín, where the megabeds are surrounded by alternating thin-bedded to medium-bedded turbidites, which show more intensive current bottom erosion. Paleocurrent data derived from these flute casts, longitudinal furrows, ridges and tool marks provide flow orientation from SW and W to NE and E. The determination of typical paleocurrent indicators from individual megabeds was difficult, since in the majority of localities their basal bottom surfaces are not visible or high-concentration flows at the base of turbidity currents did not allow the development of any current marks. Additional paleocurrent data have been identified from climbing-ripple structures in cross lamination of the megabeds (SE transport direction), grain imbrication in laminae (to E and NE), parting lineation (SW–NE orientation) and the orientation of the long axis of the pseudonodules in the CB$_C$ division (WSW–ENE orientation).

Stratigraphic position of megabeds

An important aspect of this study is the stratigraphic position of the megabeds. The biostratigraphic classification of the

megabeds has been carried out by foraminiferal and nannoplankton study of claystone intervals. The foraminiferal microfauna of these claystones consists of small-sized forms of tenuitellids, pseudohastigerinids, paragloborotalids, cassigerinelinids, chiloguembelinids and catapsydracids (see Fig. 12). They contain several index species, like *Tenuitella gemma* (Jenkins), *T. munda* (Jenkins), *T. clemenciae* (Bermudez), *T. brevispira* (Subbotina), *Pseudohastigerina micra* (Cole), *P. naguewichiensis* (Myatliuk), *Paragloborotalia nana* (Bolli), *Chiloguembelina cubensis* (Palmer), *Cassigerinella chipolensis* (Cuschman & Ponton), *Dentoglobigerina rohri* (Bolli), *Globorotaloides suteri* Bolli, *Catapsydrax martini* Blow & Banner, *Protentella* (*Bolliella*) *navazuelensis* Molina, etc., which are common in the Early Oligocene associations (see Berggren et al. 1967; Li 1987; Leckie et al. 1993; Spezzaferri 1994; Pearson & Wade 2009). The presence of *Pseudohastigerina* shows that the age of the megabeds should not be younger than the early middle Rupelian, which in the P-series zonation corresponds to the P18 Biozone (*Chiloguembelina cubensis–Pseudohastigerina* spp. sensu Berggren et al. 1995), and in the O-series zonation corresponds to the O1 Biozone (*Pseudohastigerina naguewichensis* HOZ sensu Berggren & Pearson 2005). *Tenuitella*-rich associations with other microperforate foraminifers are common in the Oligocene formations of the Carpathian Flysch units (Olszewska 1985; Bąk
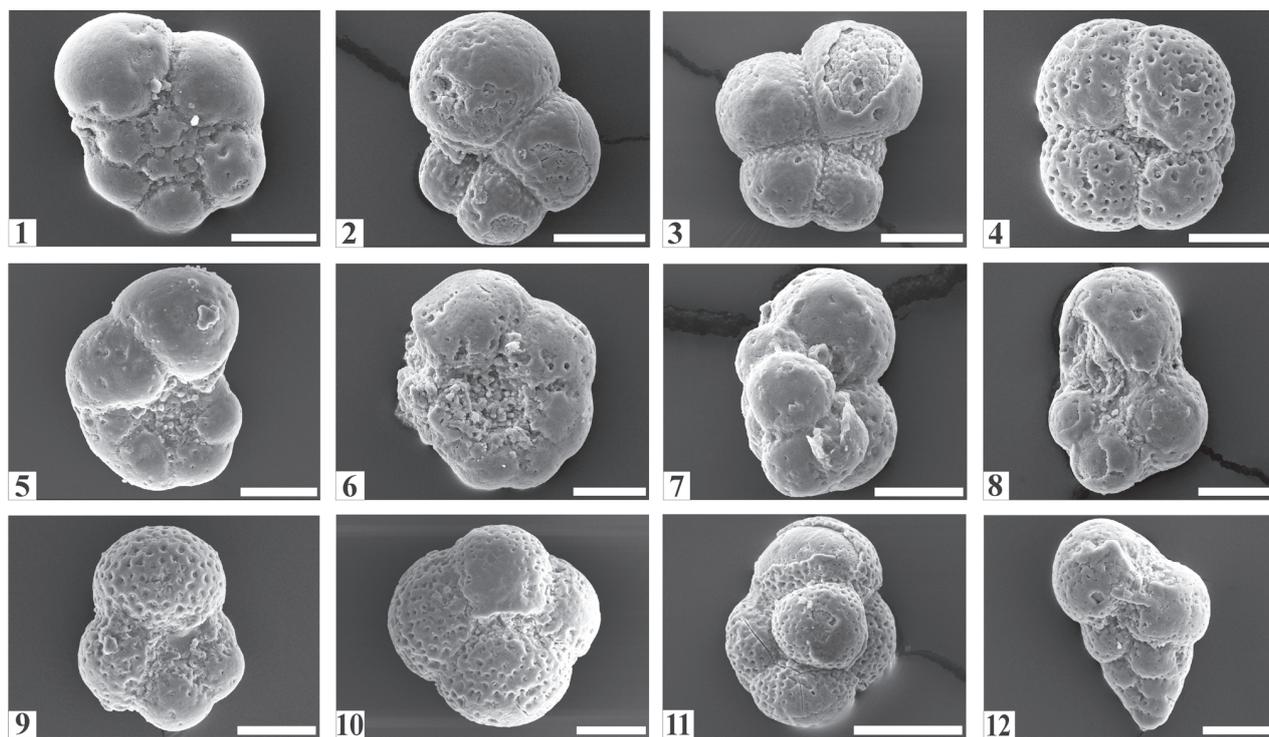

Fig. 12. Representative species of the foraminiferal microfauna from the megabeds in the Veľký Bysterec locality. **1** — *Tenuitella gemma* (Jenkins); sample DK-1, scale bar 20 μm. **2** — *Tenuitella munda* (Jenkins); sample DK-3, scale bar 50 μm. **3** — *Tenuitella clemenciae* (Bermudez); sample DK-3, scale bar 50 μm. **4** — *Paragloborotalia nana* (Bolli); sample DK-3, scale bar 40 μm. **5** — *Pseudohastigerina micra* (Cole); sample DK-1, scale bar 40 μm. **6** — *Pseudohastigerina naguewichiensis* (Myatliuk); sample DK-3, scale bar 40 μm. **7** — *Cassigerinella chipolensis* (Cuschman & Ponton), DK-4, scale bar 40 μm. **8** — *Protentella* (*Bolliella*) *navazuelensis* Molina; sample DK-2, scale bar 40 μm. **9** — *Globorotaloides suteri* Bolli; sample DK-3, scale bar 40 μm. **10** — *Dentoglobigerina rohri* (Bolli); sample DK-3, scale bar 40 μm. **11** — *Catapsydrax martini* (Blow & Branner); sample DK-3, scale bar 50 μm. **12** — *Chiloguembelina cubensis* (Palmer); sample DK-3, scale bar 40 μm.

2005; Bubík & Poul 2010, etc.). Olszewska (1997) defined their acme zones for the Rupelian–lower Chattian sediments. Dominance of tenuitellids provides evidence of cold-water condition of the Early Oligocene (e.g. Pippèrr & Reichenbacher 2010).

The foraminiferal stratigraphic data correspond to the results of the nannoplankton stratigraphy. The nannofossil associations (Fig. 13) imply the coexistence of *Transversopontis fibula* Gheta and *Reticulofenestra ornata* Müller, which is indicative for the NP23 Biozone (Nagymarosy & Voronina 1992; Krhovský et al. 1992; Švábenická et al. 2007, etc.). However, the low frequency of these species points rather to the upper part of the NP22 and lower part of the NP23 Zones. Other nannoplankton species include *Helicosphaera compacta* Bramlette & Wilcoxon, *Helicosphaera bramlettei* Müller, *Chiasmolithus oamaruensis* (Deflandre), *Isthmolithus recurvus* Deflandre, *Lanternithus minutus* Stradner, *Coccolithus formosus* (Kamptner), *Transversopontis pulcheroides* (Sullivan) and abundant reworked species of Eocene and Cretaceous nannofossils (e.g. *Discoaster barbadiensis* Tan, *Discoaster saipanensis* Bramlette, *Tribrachiathus orthostylus* (Bramlette & Riedel), *Eifellithus* sp.

The stratigraphic data obtained from the foraminiferal and nannofossil study allow us to properly determine the age of the Orava megabeds as early middle Rupelian (P18/O1–NP22/NP23 Biozones) (Fig. 14).

Discussion

Interpretation of the Orava megabeds

Sedimentological literature provides a lot of ideas concerning the processes that initiate the turbidity currents. However, displacement of enormous amounts of material in single flows is rare and megabeds, like those in the Orava region, which are characterized by great thickness, considerably exceeding the thickness of related beds in other parts of the depositional system, suggests catastrophic events on the basinal margins.

The presence of the Orava megabeds makes it possible to discuss possible paleogeographical scenarios explaining how to deliver the required volume of sediments to the Central Carpathian Paleogene Basin and confront our data with published modern analogues of such a type of megabeds. The sedimen-
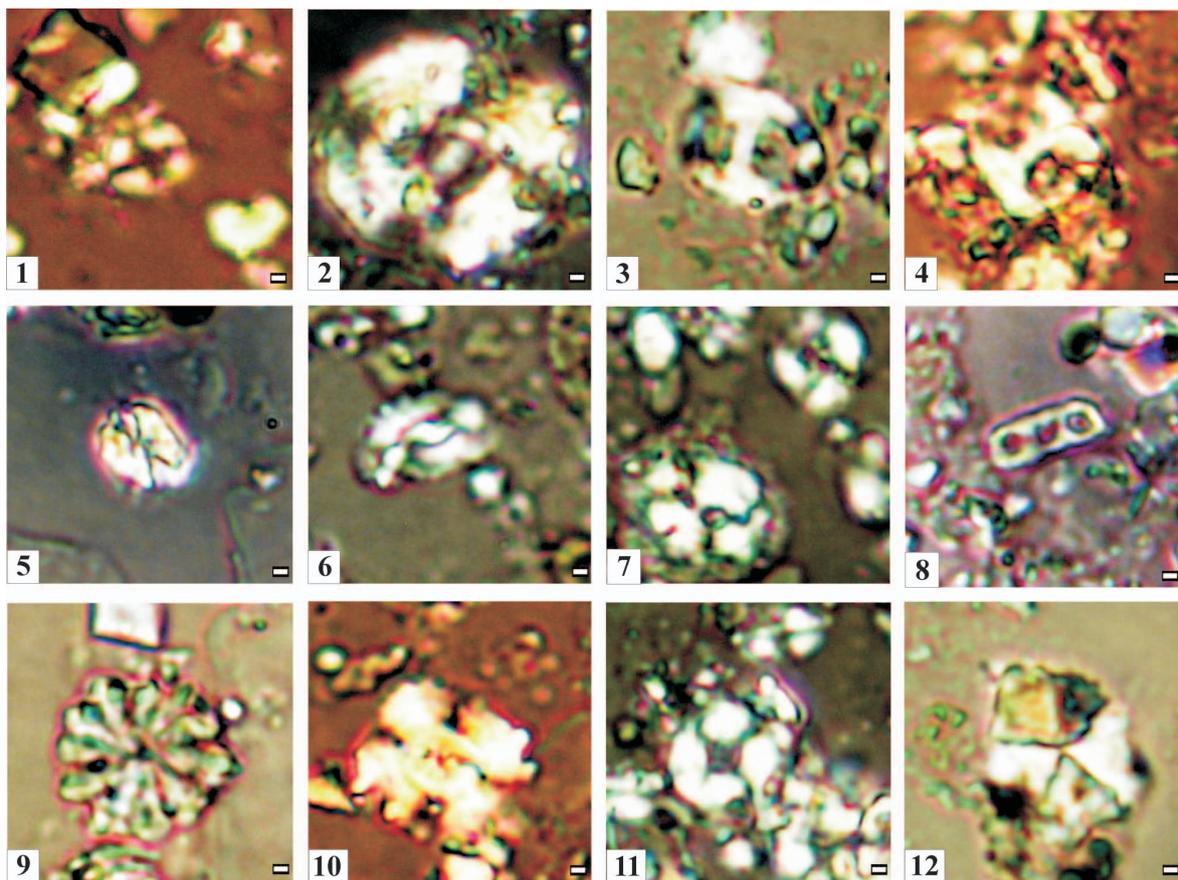

Fig. 13. Representative species of calcareous nannofossils from the megabeds in the Veľký Bysterec locality. **1** — *Reticulofenestra ornata* Müller; sample DK-1. **2** — *Reticulofenestra umbilica* (Levin); sample DK-4. **3–4** — *Transversopontis fibula* Gheta; sample DK-4. **5** — *Lanternithus minutus* Stradner; sample DK-3. **6** — *Helicosphaera bramlettei* Müller; sample DK-1. **7** — *Helicosphaera compacta* Bramlette & Wilcoxon; sample DK-3. **8** — *Isthmolithus recurvus* Deflandre; sample DK-4. **9** — *Discoaster barbadiensis* TAN; sample DK-4. **10** — *Dictyococcites bisectus* (Hay, Mohler & Wade) Bukry & Percival; sample DK-1. **11** — *Coccolithus formosus* (Kamptner) Wise; sample 4. **12** — *Braarudosphaera bigelowii* (Gran & Braarud) Deflandre; sample DK-3. Scale bar for all figures: 1 μm.
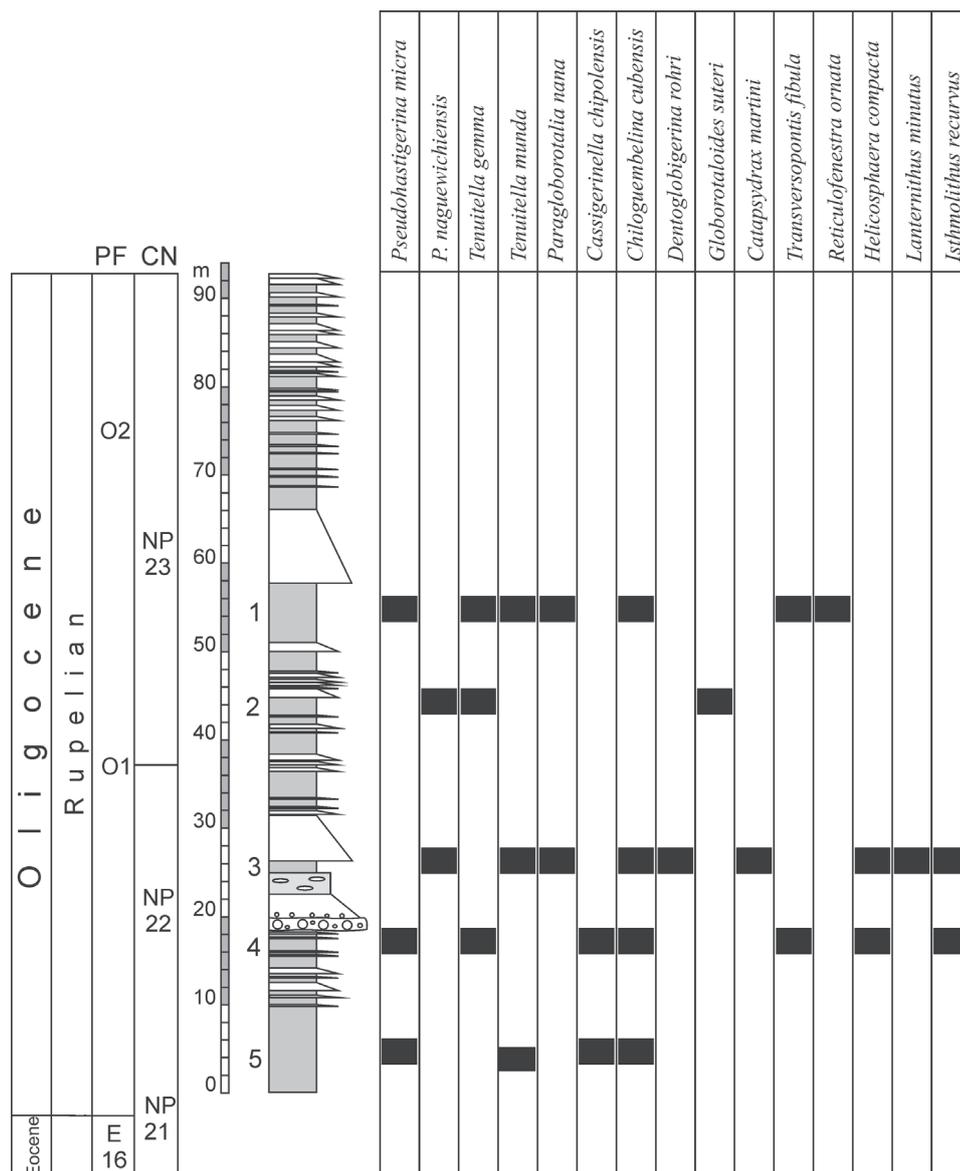
Fig. 14. Stratigraphic distribution of foraminiferal and nannofossil species in the megaturbidite sequence of the CCPB (Bysterec section). Based on the index species the age of the Orava megabeds corresponds to the Biozones O1–O2 and NP22–NP23 (early middle Rupelian). The numbers (1–5) mark the samples taking position.

only minor turbidity currents are associated with frequent failures and significant turbidity currents are only rarely created by liquefaction of sand or silt beds (e.g. Tripsanas et al. 2008; Piper & Normark 2009). Moreover, the duration of sediment liquefaction and their simple slope failures was measured in minutes or at most hours (Andresen & Bjerrum 1967; Karlsrud & Edgers 1982; De Groot et al. 1987; Emdal et al. 1996), therefore the longer lasting events of failure, capable of producing the units on the scale of the megaturbidites, could only originate by multifold steps of shoreline retrogression. Even if distributaries and fan deltas on the basinal margins could supply enough sand and silt, the coarse sediments are blanketed by the plume-type mud deposits, occurred as a thin mudstone interbeds in sandy deposits. The compaction of the mudstones could establish their resistivity to retrogression. The beds originated by successive retrogressive failures would produce abundant mudstone intraclasts, but they are entirely missing in all of the sandstone/siltstone facies of the Orava megabeds. We suppose, that probably only coarse-grained CB_A unit of the complex beds, the structures of which indicate deposition from debris flow, can be explained by slope failure from the basinal shelf-slope systems. The failures could be generated by extensive breakdowns in the delta front, but the large amount of bioclasts from the Eocene carbonates as well as the presence of synsedimentary slumps and coherent blocks suggests that not only the Oligocene deposits (mudstone intraclasts) but also unconsolidated or semiconsolidated older deposits of the Borové Formation were affected by slope failures. These failures could be connected with oceanographic processes in canyon head or with straight-sided deeply incised conduits where erosion by flows might have provided conditions for breaching (e.g. Piper & Normark 2009).

tary volume of megaturbidites is frequently used in literature for their classification as well as for interpretation of the processes that triggered these flows (e.g. Mutti et al. 1984; Reeder et al. 2000; Piper & Normark 2009). In spite of the fact that the Orava megabeds are considered to represent the deposits of large voluminous flows, their total sedimentary volume in the CCPB could not be properly quantified. Therefore, it is difficult to come to decisive hypothesis about the formation of such exceptionally thick units as the Orava megabeds, so that we provide rather a multiproxy approach to interpretation of their possible depositional mechanisms. The large voluminous gravity flows are often linked to seismic activity causing upslope slide failure (e.g. Mutti et al. 1984; Sérguret et al. 1984; Labaume et al. 1987). However, some authors suggest that

The megaturbidites, developed as several meters thick, finely structuralized sandstone and siltstone of the CB_B unit,

apparently differ from of the CB_A unit. The detrital particles of the Orava megabeds have a polygenic composition, reflecting the presence of plutonic, supracrustal, low-grade metamorphic and sedimentary rocks in the source areas. The plutonic and metamorphic sources were exposed and denuded together with the unstable rocks of the carbonate complexes. Almost 90 % of the sandstone and siltstone sediments of the megabeds are well sorted and they lack larger boulders and coarse-grained clastics. Therefore, such fine-grained sediments with mature siliciclastic composition appear to have been accumulated by rivers, which fed the basin from tectonically active sources with permanent discharge of finely disintegrated particles. The large amount of coal particles, coal seams and wood fragments in sandstone- to siltstone lithofacies of the Orava megabeds could also indicate a source in the delta deposits or fluvial discharge to the continental shelf (cf. Mutti et al. 2003). Riverine input of hyperconcentrated bedload during catastrophic floods that flowed seaward due to inertia could have generated voluminous flows which deposited very thick sandstone–siltstone beds (e.g. Mutti et al. 2000, 2003, 2009; Normark & Reid 2003; Plink-Björklund & Steel 2004; Piper et al. 2007). However, the largest observed turbidites are much more voluminous than the sediment discharge of a large single river flood (Piper & Normark 2009). Similarly, the storm-initiated deposition of turbidites are generally supply-limited because of the death of the many flows inside the canyon (Piper 1970; Paull et al. 2005) and only occasional flows become sufficiently large and energetic to reach the basin floor (e.g. Piper & Normark 1983). The channel avulsions, which occasionally occurred due to flow erosion, may also result in deposition of exceptionally thick sand beds (Piper & Normark 2001). However, such beds are usually massive, unstructured and rich in mudstone clasts, therefore they differ from structural and textural features of the sandstones in the Orava megabeds.

Even though each of these processes alone is questionable as the main generating mechanism of the Orava megabeds, they would represent effective triggers that in combination with the suitable condition on the basinal margins could led to the formation of large-scale gravity flows.

Nevertheless, the main factor which probably played a significant role in triggering of the voluminous flows is inferred in long-lasting accumulation of the clastics on the basinal margins of the CCPB.

The CCPB as a tectonic-type basin was bordered by active margins flanked by coarse-grained and sandy sediments of alluvial fan, fluvial, fluviodeltaic and fan-delta systems, which after the marine incursion fed the coastal zone (Marschalko 1970; Baráth & Kováč 1995; Filo & Siráňová 1996, 1998). Interference of eustasy and tectonics led to the relative sea-level changes in the CCPB, evolution of which involved a succession of highstand and lowstand phases with shifting of the coastline and marginal facies (e.g. Soták et al. 2001; Starek et al. 2012). During the Early Oligocene, the CCPB passed through a highstand stage of relative sea level (e.g. Soták 1998; Soták et al. 2001), when the majority of the coarse sediments remained in fan deltas and in actively prograded peripheral beaches (cf. Dabrio 1990). The coastal erosion of ravinement surfaces on the basinal margins of the

CCPB during the rise in sea-level rising from the Priabonian/early Rupelian transition, together with high-bedload riverine input into the marine realm could have produced a large quantity of sediments, which were delivered to conduit heads through longshore drift, or fan delta progradation and subsequently remobilized by following initiating processes (e.g. Piper & Normark 2001).

Even though hyperpycnal flows generated by catastrophic floods are questionable as initiating events of the Orava megabeds, their deposition would be influenced by these processes as well. These large-volume and highly turbulent flows could have accelerated down the continental slopes, eroding deposits from the conduit and basinal-slope accumulations, progressively increasing the proportion of sand in the flows, which were transported a significant distance onto the basin floor (e.g. Hughes Clarke et al. 1990; Piper & Normark 2001, 2009; Talling et al. 2007). Downslope passing of the large highly erosive hyperpycnal flows could have been accompanied by extensive slope failures of straight-sided deeply incised conduits, which could have led to initiation of debris flows at the base of the complex beds resulting in highly disorganized deposit (C_1 subfacies) frozen during the early stages of their downslope motion. Disorganized pebbly mudstone facies and massive conglomerates (debris-flow deposits or debrites) at the base of thick sandy/silty beds characterized by a fining upward facies sequence (turbulent portions of the flow) are referred to as highly efficient bipartite flows (e.g. Mutti et al. 2003; Tinterri et al. 2003) in which sharp grain-size breaks represent a variation in hydrodynamic conditions of the gravity flow during its downcurrent evolution.

The CB_B unit, as well as the unit identified as megaturbidites, which probably represent the more distal equivalents of the composite megabeds, were produced during a single event and reflect the continual deposition from the turbulent flows. Their structures suggest basal near bed processes as follows: — rapid deposition of coarse-grained sediments from high-concentration flow at the base of the turbidity currents (C_{2-3}, S_{1-2} subfacies); — steady basal shear stress (growth and collapse in the traction carpets) and a steady rain of suspended sediment (S_{3-7}, Si_{1-3} subfacies); — intermittent phases of variable flow velocity (S_4, S_5 subfacies); — successive decreases in flow competence (upwardly-fining granulometry) and terminal depositional processes from muddy suspension (M lithofacies). The rapid deposition of the megabeds is expressed by the water escape structures and hydroplastic deformations (S_{6-7}, Si_3 subfacies).

The megabeds with a great thickness (>1 m) and similar alteration of plane-parallel lamination with climbing ripple lamination, and with large amounts of coal seams and wood fragments could be interpreted as deposits from hyperpycnal flows (e.g. Mutti et al. 2003; Olariu et al. 2010).

The period of long-lasting proximal deposition and lower frequency of catastrophic events due to low activity of triggering mechanisms, and following conduit flushing appears to have been the most common source of sediment for very large turbidites. Conduit flushing could explain why the volume of megaturbidites is much greater than the volume of sediments transported in a single river flood or from usual

slope failures (Piper & Normark 2009), which is probably the case of the sediments in the Orava megabeds.

Deposition from turbidity currents played an important role in basin-forming processes of the CCPB, where the turbidite systems were influenced mainly by tectonics and eustacy (e.g. Soták 1998; Starek et al. 2000; Soták et al. 2001; Starek 2001). However, only one of the sedimentary formations of the CCPB reveals the occurrence of overthickened sandstone–siltstone beds without internal erosive surfaces or amalgamation surfaces as well as grain-size breaks, which therefore should be deposit from single depositional events.

The early stages of deposition in the CCPB revealed mainly continental and shallow-marine conditions, when after the initial transgression (TA3.5–3.6 third-order Exxon cycles), the subaerial sediments changed to subaqueous sediments in the Borové Formation (Baráth & Kováč 1995). This formation comprises mainly deposits of alluvial fans, fluvial and fluviodeltaic systems, fan-deltas as well as shoreface and carbonate ramp environments (Marschalko 1970; Kulka 1985; Baráth & Kováč 1995; Filo & Siráňová 1996, 1998; Janočko & Jacko 1998; Soták et al. 2001). The distinctive eustatic fall of sea level in the early Priabonian at the beginning of the TA4 supercycle led to regression, subaerial exposure and erosion of the Middle Eocene formations. The exposed shelf was prone to developing incised valleys as a result of fluvial erosion (Starek et al. 2012). During the Priabonian transgression, the subsequent rise of the relative sea level accompanied by rapid tectonic subsidence along the fault-bounded margins of the CCPB (Soták et al. 2001) led to extensive flooding and deepening of depositional environments (e.g. Buček et al. 1998). In this stage of the basin's evolution, most of the clastics, produced by rivers and erosion of flooded land, was retained on the coastal plain as a component of beach complexes and deltaic systems. Direct riverine sediment-laden discharge to the distal parts of the basin is rather rare. The large volume of sand could be trapped within incised-conduit heads and delta distributaries.

During the late Priabonian and Rupelian, the CCPB was filled up by mud-rich deposits of the Huty Formation, which represents different sediments of the deep-marine clastic systems (e.g. Janočko & Jacko 1999; Soták et al. 2001; Starek et al. 2004). In the lower part of the Huty Formation the mudstones greatly prevail over sandstones. The sandy turbidites, in dependence on their position in the submarine turbidite systems, mostly do not exceed a thickness of 10 cm, only rarely reaching up to 50 cm. These deposits of the Huty Formation are associated with the Orava megabeds, the possible initiating mechanisms of which are discussed above. However, numerous sandy turbidites are generated during falling sea-level stages, which result in progradation and cannibalization of the fan delta (e.g. Postma 1995) and as the major riverine input of sediment-laden flows occur seaward of high bedload deltas (e.g. Milliman & Kao 2005; Normark et al. 2006; Milliman et al. 2007). Evidence of the large-volume hyperpycnal-type sediments in submarine turbidite deposits of the CCPB may indicate the transitional sea-level drop during the early Rupelian, which culminated by riverine input, brackishing and semiisolation in the NP23 Zone (Soták 2010).

Incoming regression of the TB1 supercycle in the CCPB, which resulted from an abrupt sea-level fall at around 30 Ma at a time of major glaciation in Antartica (Robin 1988; Kennett & Barker 1990; Zachos et al. 1993), led to sand-rich submarine fan deposition of the Zuberec and Biely Potok Formations (Soták 1998; Soták & Starek 1999; Starek et al. 2000). These Upper Oligocene formations show an abundance of thick sandstone beds, especially the sandstone lithosomes of the Biely Potok Formation up to several meters in thickness. Their coalescing lobes grade up to form the mid-fan lobe complex. However, the thick tabular sandstones of the Biely Potok Formation are amalgamated from units, usually up to 1 m thick beds (Gross et al. 1993; Starek 2001), which are usually massive, unstructured and contain abundant claystone chips. Unlike the Orava megabeds, these sandstones are laminated only in the topmost part of the beds. In spite of a good predisposition of basin margins for initiation of sandy turbidites during the Late Oligocene regression in the CCPB, their triggering frequency probably did not allow long-lasting accumulation of sandy sediments, which would be sufficient to generate such large-volume gravity flows like those, which delivered such a volume of sand to the megabeds in the lower part of the Huty Formation.

Conclusion

The Orava megabeds provide a record of major depositional events in the western part of the Central Carpathian Paleogene Basin (CCPB). They are specific for certain development stage of this basin, because of their occurrence only in the lower part of the Huty Formation, where they form distinct interval with far-reaching correlation over tens of kilometers within the basin fill. The megabeds occur in the middle Rupelian sequence, the biostratigraphic age of which, derived from foraminifers and nannofossils, corresponds to P18/O1 and NP22/23 Biozones.

Two types of megabeds, slightly dissimilar in their sedimentary features and flow-type deposition were classified here. They are developed as separated beds (megaturbidites) and the complex beds (CB). The megaturbidites are represented by thick finely structured beds with upwardly-fining trend in grain size from fine-grained conglomerates and sandstones to siltstones and homogeneous mudstones. The complex beds include a basal disorganized coarse-grained unit (CB_A); heterolithic unit equivalent to the megaturbidite (CB_B); and the mixed lithofacies of deformed sandy/silty claystones (CB_C).

The complex beds can be interpreted as a result of bipartite flows (e.g. Mutti et al. 2003; Tinterri et al. 2003) with debris-flow deposit at the base, and with superincumbent thick finely structured sandstone/siltstone facies resulting from turbulent portions of the flow. Individually placed megaturbidites probably represent the more distal equivalents of the complex beds and reflect uninterrupted deposition from turbulent flows.

We suppose, that two main factors probably played significant roles in the generation of the large-volume gravity flows and deposition of the Orava megabeds in the middle Rupelian sequence of the CCPB.

1. Long-lasting accumulation of the clastics on the basinal margins of the CCPB during a period of rising sea-level and a highstand stage of relative sea level in the early Rupelian.

2. The catastrophic trigerring mechanisms on the basinal margins which could have led to the formation of large-scale gravity flows.

Several triggers, including oceanographic processes in a canyon head or upslope slide failures linked with seismic activity could have initiated these processes, and therefore we cannot definitely exclude them. However, the basin-scale extension forming a coeval horizon of sandstone megabeds; finely structured sandstone/siltstone facies with definite plane-parallel stratification and climbing ripple lamination; differences between shelf-derived carbonate material in the basal part of complex beds and continental-derived sandy/silty siliciclastic material of the megaturbidites as well as a great abundance of continental material (phytodetritus, leaves) suggest that deposition of the Orava megabeds was influenced by erosive hyperpycnal flows generated by catastrophic floods.

The presence of hyperpycnal deposits in the CCPB could indicate the connection of the turbidite systems of deep-sea fans with fluvial systems and shelf-edge deltas, which is a new insight in the reconstruction of this basin. The occurrence of megabeds in the lower part of the Huty Formation provide evidence of possible rising discharge from flooding rivers, which entered the CCPB from the SW and W to NE and E.

Flood discharge and generation of hyperpycnal flows with deposition in deep-sea should be dominant processes during a sea-level fall and the extremely large volume of clastics in the megabeds could be derived by conduit flushing and coastal erosion of deposits accumulated in shelf areas during previous rising of the sea level. It is probably also a case of hyperpycnal megaturbidites in the CCPB, where their accumulation followed the sea-level highstand in the Globigerina Marls at the Eocene/Oligocene boundary and fall to the sea-level lowstand during the early Rupelian, which culminated in riverine input, brackishing and semi-isolation in the NP23 Zone.

References

Abreu V.S. & Haddad G.A. 1998: Glacioeustatic fluctuations: the mechanism linking stable isotope events and sequence stratigraphy from the Early Oligocene to Middle Miocene. In: de Graciansky P.-C., Hardenbol J., Jacquin T. & Vail P.R. (Eds.): Mesozoic and Cenozoic sequence stratigraphy of European basins. *SEPM, Spec. Publ.* 60, 245–259.

Allen J.R.L. 1970: A quantitative model of climbing ripples and their cross-laminated deposits. *Sedimentology* 14, 5–26.

Anastasakis G. 2007: The anatomy and provenance of thick volcani-

clastic flows in the Cretan Basin, South Aegean Sea. *Mar. Geol.* 240, 113–135.

Anastasakis G. & Pe-Piper G. 2006: An 18 m thick volcaniclastic interval in Pantelleria Trough, Sicily Channel, deposited from a large gravitative flow during the Green Tuff eruption. *Mar. Geol.* 231, 201–219.

Andresen A. & Bjerrum L. 1967: Slides in subaqueous slopes in loose sands and silts. In: Richards A.F. (Ed.): Marine geotechnique. *University of Illinois Press*, Urbana, 221–239.

Baráth I. & Kováč M. 1995: Systematics of gravity-flow deposits in the marginal Paleogene formations between Markušovce and Kluknava villages (Hornád Depression). *Miner. Slovaca, Geovest.* 27, 1, 6.

Bartholdy J., Bellas S.M., Cosovic V., Fucek V.P. & Keupp H. 1999: Processes controlling Eocene mid-latitude larger Foraminifera accumulations: modelling of the stratigraphic architecture of a fore-arc basin (Podhale Basin, Poland). *Geol. Carpathica* 50, 6, 435–448.

Bąk K. 2005: Foraminiferal biostratigraphy of the Egerian flysch sediments in the Silesian nappe, Outer Carpathians, Polish part of the Bieszczady Mountains. *Ann. Soc. Geol. Pol.* 75, 71–93.

Berggren W.A. & Pearson P.N. 2005: A revised tropical to subtropical Paleogene planktonic foraminiferal zonation. *J. Foram. Res.* 35, 4, 279–298.

Berggren W.A., Olsson R.K. & Reyment R.A. 1967: Origin and development of the foraminiferal genus *Pseudohastigerina* Banner & Blow, 1959. *Micropaleontology* 13, 3, 265–288.

Berggren W.A., Kent D.V., Swisher C.C. III. & Aubry M.P. 1995: A revised Cenozoic geochronology and chronostratigraphy. In: Berggren W.A., Kent D.V., Aubry M. & Hardenbol J. (Eds.): Geochronology, time scales and global correlation. *SEPM, Spec. Publ.* 54, 129–212.

Best J.L. & Bridge J.S. 1992: The morphology and amplitude of low amplitude bedwaves upon upper-stage plane beds and the preservation of planar laminae. *Sedimentology* 39, 737–752.

Biely A., Bezák V., Elečko M., Kaličiak M., Konečný V., Lexa J., Mello J., Nemčok J., Potfaj M., Rakús M., Vass D., Vozár J. & Vozárová A. 1996: Geological map of Slovakia (1:500,000). *Geological Survey of Slovak Republic*, Bratislava.

Blair T.C. & McPherson J.G. 1999: Grain-size and textural classification of coarse sedimentary particles. *J. Sed. Res.* 69, 1, 6–19.

Bouma A.H. 1962: Sedimentology of some flysch deposits. *Elsevier* Amsterdam, 1–168.

Bouma A.H. 1987: Megaturbidite: an acceptable term? *Geo-Mar. Lett.* 7, 63–67.

Bubík M. & Poul I. 2010: Sediments of the Pouzdřany Unit in the HV-1 well Dolní Věstonice. *Zpr. Geol. Výzk. v Roce 2009*, 16–18.

Buček S., Salaj J., Köhler E. & Gross P. 1998: A sudden deepening of the Central Western Carpathian area in the Upper Eocene. *Zem. Plyn Nafta* 43, 1, 173–177.

Bugge T., Befring S., Belderson R.H., Eidvin T., Jansen E., Kenyon N.H., Holtedahl H. & Sejrup H.P. 1987: A threestage submarine slide off Norway. *Geo-Mar. Lett.* 7, 191–198.

Bugge T., Belderson R.H. & Kenyon N.H. 1988: The Storegga slide. *Roy. Soc. (London), Philosophical Trans.* 325, 357–388.

Carter L., Milliman J.D., Talling P.J., Gavey R. & Wynn R.B. 2012: Near-synchronous and delayed initiation of long run-out submarine sediment flows from a record-breaking river flood, offshore Taiwan. *Geophys. Res. Lett.* 39, L12603, Doi:10.1029/2012GL051172

Cita M.B., Camerlenghi A., Kastens K.A. & McCoy F.W. 1984: New findings of the Bronze age Homogenites in the Ionian Sea: geodynamic implications for the Mediterranean. *Mar. Geol.* 55, 47–62.

Cita M.B., Camerlenghi A. & Rimoldi B. 1996: Deep sea tsunami

deposits in the eastern Mediterranean: new evidence and depositional models. *Sed. Geol.* 104, 155–173.

Csontos L., Nagymarosy A., Horváth F. & Kováč M. 1992: Tertiary evolution of the Intra-Carpathian area: a model. *Tectonophysics* 208, 1–3, 221–241.

Dabrio C.J. 1990: Fan-delta facies associations in Late Neogene and Quaternary basins of southeastern Spain. In: Colella A. & Prior D.B. (Eds.): Coarse-grained deltas. *Int. Assoc. Sed., Spec. Publ.* 10, 91–111.

Davies N.S., Turner P. & Sansom I.J. 2004: Soft-sediment deformation structures in the Late Silurian Stubdal Formation: the result of seismic triggering. *Norwegian J. Geol.* 1, 85, 233–243.

De Groot M.B., Silvis F., van Rossum H. & Koster M.J. 1987: Liquefied sand flowing over a gentle slope. In: Hanrahan E.T., Orr T.L.L. & Widdis T.F. (Eds.): Proceedings IXth European Conference on Soil Mechanics and Foundation Engineering. *Balkema*, Rotterdam 2, 595–598.

Doyle L.J. 1987: Anomalously large marine sedimentary units deposited in a single mass wasting event. *Geo-Mar. Lett.* 7, 2, 59–61.

Doyle L.J. & Bourrouilh R. 1986: Carbonate megaturbidites — examples from the Gulf of Mexico and the French Pyrenees. *Amer. Assoc. Petrol. Geol. Bull.* 70, 583.

Dypvik H. & Jansa L. 2003: Sedimentary signatures and processes during marine bolide impacts: a review: *Sed. Geol.* 161, 309–337.

Emdal A., Janbu N. & Sand K. 1996: The shoreline slide at Lade. In: Senneset Y. (Ed.): Landslides. *Balkema*, Rotterdam, 533–538.

Filo I. & Siráňová Z. 1996: The Tomášovce Member — a new lithostratigraphic unit of the Subtatric Group. *Geol. Práce, Spr.* 102, 41–49.

Filo I. & Siráňová Z. 1998: Hornád and Chrasť Member — new regional lithostratigraphic units of the Sub-Tatric Group. *Geol. Práce, Spr.* 103, 35–51.

Fukushima Y., Parker G. & Pantin H.M. 1985: Prediction of ignitive turbidity currents in Scripps submarine canyon. *Mar. Geol.* 67, 55–81.

Gedl P. 2000: Biostratigraphy and palaeoenvironment of the Podhale Palaeogene (Inner Carpathians, Poland) in the light of palynological studies. *Stud. Geol. Pol.* 117, 155–303.

Gee M.J.R., Gawthorpe R.L. & Friedmann S.J. 2006: Triggering and evolution of a giant Submarine Landslide, Offshore Angola, Revealed by 3D seismic stratigraphy and geomorphology. *J. Sed. Res.* 76, 1, 9–19.

Ghibaudo G. 1992: Subaqueous sediment gravity flow deposits: practical criteria for their field description and classification. *Sedimentology* 39, 423–454.

Golab J. 1959: On the geology of the western Podhale flysch area. *Biul. Inst. Geol.,* Warszawa, 1–149.

Gross P., Köhler E. & Borza K. 1982: Conglomerate submarine fans from the Central-Carpathians Paleogene near Pucov. *Geol. Práce, Spr.* 77, 75–86.

Gross P., Köhler E. & Samuel O. 1984: A new lithostratigraphic subdivision of the Central Carpathian Paleogene. *Geol. Práce, Spr.* 81, 103–117.

Gross P., Köhler E., Mello J., Haško J., Halouzka R. & Nagy A. 1993: Geology of Southern and Eastern Orava. *D. Štúr Inst. Geol.*, Bratislava, 1–292.

Haq B.U., Hardenbol J. & Vail P.R. 1988: Mesozoic and Cenozoic chronostratigraphy and cycles of sea-level change. In: Wilgus C.K., Hastings B.S., Ross C.A., Posamentier H., van Wagoner & Kendall C.G. (Eds.): Sea-level changes: an integrated approach. *SEPM, Spec. Publ.* 42, 71–108.

Hein F.J. & Syvitski J.P.M. 1992: Sedimentary environments and facies in an arctic basin, Itirbilung Fiord, Baffin Island, Canada. *Sed. Geol.* 81, 17–45.

Hieke W. 1984: A thick Holocene homogenite from the Ionian Abyssal Plain (Eastern Mediterranean). *Mar. Geol.* 55, 63–78.

Hiscott R.N. 1994: Traction-carpet stratification in turbidites — fact or fiction? *J. Sed. Res.* A64, 204–208.

Hughes Clarke J.E., Shor A.N., Piper D.J.W. & Mayer L.A. 1990: Large scale current-induced erosion and deposition in the path of the 1929 Grand Banks turbidity current. *Sedimentology* 37, 613–629.

Iturralde-Vinent M.A. 1992: A short note on the Cuban late Maastrichtian megaturbidite (an impact-derived deposit?). *Earth Planet. Sci. Lett.* 109, 225–228.

Janočko J. & Jacko S. 1999: Marginal and deep-sea deposits of Central-Carpathian Paleogene Basin, Spiš Magura region, Slovakia: implication for basin history. *Slovak Geol. Mag.* 4, 4, 281–292.

Janočko J. & Jacko S. Jr. 2001: Turbidite deposit systems of the Central-Carpathian Paleogene Basin. *GeoLines* 13, 133–140.

Janočko J., Hamršmíd B., Jacko S. & Siráňová Z. 1998: Suprafan and channel — and levee deposits at Tichý Potok section, Levoča Mts.; Central Carpathian Paleogene Basin, Slovakia. *Slovak Geol. Mag.* 4, 1, 3–15.

Johnson K.S., Paull C.K., Barry J.P. & Chavez F.P. 2001: A decadal record of underflows from a coastal river into the deep sea. *Geology* 29, 1019–1022.

Jopling A.V. & Walker R.G. 1968: Morphology and origin of ripple-drift cross-lamination, with examples from the Pleistocene of Massachusetts. *J. Sed. Petrology* 38, 971–984.

Karlsrud R. & Edgers L. 1982: Some aspects of submarine slope stability. In: Saxov S. & Nieuwenhuis J.K. (Eds.): Marine slides and other mass movements NATO conference series IV, Marine sciences. *Plenum*, New York 6, 61–81.

Kennett J.P. & Barker P.F. 1990: Latest Cretaceous to Cenozoic climate and oceanographic developments in the Weddell Sea, Antarctica: an ocean-drilling perspective. *Proceedings of the Ocean Drilling Program, Scientific Results* 113, 937–960.

Krhovský J., Adamová J., Hladíková J. & Maslowská H. 1992: Paleoenvironmental changes across the Eocene/Oligocene, boundary in the Ždánice and Pouzdřany units (Western Carpathians, Czechoslovakia): the long-term trend and orbitally forced changes in calcareous nannofossil assemblages. In: Hamršmíd B. & Young J. (Eds.): Nannoplankton Research. *Knihovnička ZPN 14b* 2, 105–187.

Kuenen P.H. 1958: Experiments in geology. *Geol. Mag.* 23, 1–28.

Kulka A. 1985: Arni sedimentological model in the Tatra Eocene. *Geol. Quart.* 29, 31–64.

Labaume P., Mutti E. & Seguret M. 1987: Megaturbidites: a depositional model from the Eocene of the SW Pyrenean Foreland Basin, Spain. *Geo-Mar. Lett.* 7, 91–101.

Lastras G., Canals M., Hughes-Clarke J.E., Moreno A., De Batist M., Masson D.G. & Cochonat P. 2002: Seafloor imagery from the BIG'95 debris flow, western Mediterranean. *Geology* 30, 871–874.

Leckie M.R., Farnham CH. & Schmidt M.G. 1993: Oligocene planktonic foraminifer biostratigraphy of hole 803D (Ontong Java Plateau) and hole 628A (Little Bahama Bank), and comparison with the southern high latitudes. *Procceedings of the Ocean Drilling Program, Scientific Results* 130, 113–136.

Li Q. 1987: Origin, phylogenetic development and systematic taxonomy of the *Tenuitella* plexus (Globigerinitidae, Globigerininina). *J. Foram. Res.* 17, 4, 298–320.

Lowe D.R. 1975: Water escape structures in coarse grained sediments. *Sedimentology* 22, 157–204.

Lowe D.R. 1976: Subaqueous liquefied and fluidized sediment flows and their deposits. *Sedimentology* 23, 285–308.

Lowe D.R. 1982: Sediment gravity flows. II. Depositional models with special reference to the deposits of high-density turbidity currents. *J. Sed. Petrology* 52, 279–297.

Lowe D.R. & Guy M. 2000: Slurry-flow deposits in the Britannia Formation (Lower Cretaceous), North Sea: a new perspective on the turbidity current and debris flow problem. *Sedimentology* 47, 31–70.

Lowe D.R. & LoPiccolo R.D. 1974: The characteristics and origins of dish and pillar structures. *J. Sed. Petrology* 44, 484–501.

Lrnne I. & Nemec W. 2004: High-arctic fan delta recording deglaciation and environmental disequilibrium. *Sedimentology* 51, 553–589.

Marjanac T. 1996: Deposition of megabeds (megaturbidites) and sea-level change in a proximal part of the Eocene-Miocene flysch of central Dalmatia (Croatia). *Geology* 24, 543–546.

Marschalko R. 1970: The research of sedimentary textures, structures, and palaeocurrent analysis of basal formations (Central Western Carpathian Paleogene, N of Spišsko-gemerské rudohorie Mts.). *Acta Geol. Geograph. Univ. Comenianae*, *Geol.* 19, 129–163.

Masson D.G., Huggett Q.J. & Brunsden D. 1993: The surface texture of the Saharan Debris Flow and some speculations on submarine debris flow processes. *Sedimentology* 40, 583–598.

Maurya D.M., Rachna R. & Chamyal L.S. 1998: Seismically induced deformational structures (seismites) from the Mid-Late Holocene Terraces, Lower Mahi Valley, Gujarat. *J. Geol. Soc. India* 51, 755–758.

McKee E.D. 1939: Some types of bedding in the Colorado River delta. *J. Geol.* 47, 64–81.

McKee E.D. 1965: Experiments on ripple lamination. In: Middleton G.V. (Ed.): Primary sedimentary structures and their hydrodynamic interpretation. *SEPM, Spec. Publ.* 12, 66–83.

Milliman J.D. & Kao S.J. 2005: Hyperpycnal discharge of fluvial sediment to the ocean: Impact of super-typhoon Herb (1996) on Taiwanese rivers: *J. Geol.* 113, 285–299.

Milliman J.D., Lin S.W., Kao S.J., Liu J.P., Liu C.S., Chiu J.K. & Lin Y.C. 2007: Short-term changes in seafloor character due to flood-derived hyperpycnal discharge: Typhoon Mindulle, Taiwan, July 2004. *Geology* 35, 779–782.

Mitchell N.C. 2005: Channelled erosion through a marine dump site of dredge spoils at the mouth of the Puyallup River, Washington State, USA. *Mar. Geol.* 220, 131–151.

Mohrig D. & Marr J.G. 2003: Constraining the efficiency of turbidity current generation from submarine debris flows and slides using laboratory experiments. *Mar. Petrol. Geol.* 20, 883–899.

Moretti M., Alfaro P., Caselles O. & Canas J.A. 1999: Modelling seismites with a digital shaking table. *Tectonophysics* 304, 369–383.

Mulder T. & Alexander J. 2001: The physical character of subaqueous sedimentary density flows and their deposits. *Sedimentology* 48, 269–299.

Mulder T. & Syvitski J. 1995: Turbidity currents generated at river mouths during exceptional discharges to the World Oceans. *J. Geol.* 103, 285–299.

Mutti E. 1992: Turbidite sandstones. San Donato Milanese. *AGIP, Istituto di Geologia, Universita' di Parma*, 1– 275.

Mutti E., Ricci Lucchi F., Seguret M. & Zanzucchi G. 1984: Seismoturbidites: a new group of resedimented deposits. *Mar. Geol.* 55, 103–116.

Mutti E., Tinterri R., Di Biase D., Fava L., Mavilla N., Angella S. & Calabrese L. 2000: Delta-front associations of ancient flood-dominated fluvio-deltaic systems. *Rev. Soc. Geol. España* 13, 2, 165–190.

Mutti E., Tinterri R., Benevelli G., Di Biase D. & Cavanna G. 2003: Deltaic, mixed and turbidite sedimentation of ancient foreland basins. *Mar. Petrol. Geol.* 20, 733–755.

Mutti E., Bernoulli D., Ricci Lucchi F. & Tinterri R. 2009: Turbidites and turbidity currents from alpine flysch to the exploration of continental margins. *Sedimentology* 56, 267–318.

Muzzi Magalhaes P. & Tinterri R. 2010: Stratigraphy and depositional setting of Slurry and Contained (Reflected) Beds in the Marnoso-arenacea Formation (Langhian-Serravallian) Northern Apennines, Italy. *Sedimentology* 57, 1685–1720.

Nagymarosy A. & Voronina A.A. 1992: Calcareous nannoplankton from the Lower Maykopian beds (Early Oligocene, Union of Independant States). In: Hamršmíd B. & Young J. (Eds.): Nannoplankton Research. *Knihovnička ZPN, 14b* 2, 189–221.

Neuwerth R., Suter F., Guzman C.A. & Gorin G.E. 2006: Soft-sediment deformation in a tectonically active area: The Plio-Pleistocene Zarzal Formation in the Cauca Valley (Western Colombia). *Sed. Geol.* 186, 67–88.

Normark W.R. & Piper D.J.W. 1991: Initiation processes and flow evolution of turbidity currents: implications for the depositional record. In: Osborne R.H. (Ed.): From Shoreline to Abyss. *SEPM, Spec. Publ.* 46, 207–230.

Normark W.R. & Reid J.A. 2003: Extensive deposits of the Pacific Plate from Late Pleistocene North American glacial lake outbursts. *J. Geol.* 111, 617–637.

Normark W.R., Piper D.J.W. & Sliter R. 2006: Sea-level and tectonic control of middle to late Pleistocene turbidite systems in Santa Monica Basin, offshore California. *Sedimentology* 53, 867–897.

Olariu C., Steel R. & Petter A.L. 2010: Delta-front hyperpycnal bed geometry and implications for reservoir modeling: Cretaceous Panther Tongue delta, Book Cliff, Utah. *AAPG Bull.* 94, 6, 819–845.

Olszewska B. 1985: Foraminifera of the Menilite Beds (Polish External Carpathians). *Ann. Soc. Geol. Pol.* 55, 1, 2, 201–250.

Olszewska B. 1997: Foraminiferal biostratigraphy of the Polish Outer Carpathians: a record of basin geohistory. *Ann. Soc. Geol. Pol.* 67, 325–337.

Olszewska B.W. & Wieczorek J. 1998: The Paleogene of the Podhale Basin (Polish Inner Carpathians) — micropaleontological perspective. *Przegl. Geol.* 46, 721–728.

Owen G. 1987: Deformation processes in unconsolidated sands. In: Jones M.E. & Preston R.M.F. (Eds.): Deformation of sediments and sedimentary rocks. *Geol. Soc. London, Spec. Publ.* 29, 11–24.

Owen G. 1996: Experimental soft-sediment deformation: structures formed by the liquefaction of unconsolidated sands and some ancient examples. *Sedimentology* 43, 279–293.

Pauley J.C. 1995: Sandstone megabeds from the Tertiary of the North Sea. In: Hartley A.J. & Prosser D.J. (Eds.): Characterization of Deep Marine clastic systems. *Geol. Soc. Spec. Publ.* 94, 103–114.

Paull C.K., Mitts P., Ussler W., Keaten R. & Greene H.G. 2005: Trail of sand in upper Monterey Canyon, offshore California. *Geol. Soc. Amer. Bull.* 117, 1134–1145.

Pearson P.N. & Wade B.G. 2009: Taxonomy and stable isotope paleoecology of well-preserved planktonic foraminifera from the Uppermost Oligocene of Trinidad. *J. Foram. Res.* 39, 3, 191–217.

Piper D.J.W. 1970: Transport and deposition of Holocene sediment on La Jolla deep sea fan, California. *Mar. Geol.* 8, 211–227.

Piper D.J.W. 1978: Turbidite muds and silts on deep-sea fans and abyssal plains. In: Stanley D.J. & Kelling G. (Eds.): Sedimentation in submarine Canyons, fans and Trenches. *Dowden, Hutchinson and Ross*, Stroudsburg, 163–176.

Piper D.J.W. & Normark W.R. 1983: Turbidite depositional patterns and flow characteristics, Navy Submarine Fan, California Borderland. *Sedimentology* 30, 681–694.

Piper D.J.W. & Normark W.R. 2001: Sandy fans from Hueneme to Amazon and beyond. *Amer. Assoc. Petrol. Geol., Bull.* 85, 1407–1438.

Piper D.J.W. & Normark W.R. 2009: Processes that initiate turbidity

currents and their influence on turbidites: A marine geology perspective. *J. Sed. Res.* 79, 347–362.

Piper D.J.W., Shor A.N. & Hughes-Clarke J.E. 1988: The 1929 Grand Banks earthquake, slump and turbidity current. In: Clifton H.E. (Ed.): Sedimentologic consequences of convulsive geologic events. *Geol. Soc. Amer.*, *Spec. Pap.* 229, 77–92.

Piper D.J.W., Cochonat P. & Morrison M. 1999: Sidescan sonar evidence for progressive evolution of submarine failure into a turbidity current: the 1929 Grand Banks event. *Sedimentology* 46, 79–97.

Piper D.J.W., Shaw J. & Skene K.I. 2007: Stratigraphic and sedimentological evidence for late Wisconsinan subglacial outburst floods to Laurentian Fan. *Palaeogeogr. Palaeoclimatol. Palaeoecol.* 246, 101–119.

Pippèrr M. & Reichenbacher B. 2010: Foraminifera from the borehole Altdorf (SE Germany): proxies from Ottnangian (early Miocene) palaeoenvironments of the Central Paratethys. *Palaeogeogr. Palaeoclimatol. Palaeoecol.* 289, 62–80.

Plink-Björklund P. & Steel R.J. 2004: Initiation of turbidity currents: outcrop evidence for hyperpycnal flow turbidites. *Sed. Geol.* 165, 29–52.

Postma G. 1995: Sea-level-related architectural trends in coarse-grained delta complexes. *Sed. Geol.* 98, 1–4, 3–12.

Potfaj M. 1998: Geodynamics of the Klippen Belt and Flysch belt in the Western Carpathians. In: Rakús M. (Ed.): Geodynamic development of the Western Carpathians. *Dionýz Štúr Publ.*, Bratislava, 143–154.

Powers M.C. 1953: A new roundness scale for sedimentary particles. *J. Sed. Petrology* 23, 117–119.

Prior D.B. & Bornhold B.D. 1989: Submarine sedimentation on a developing Holocene fan delta. *Sedimentology* 36, 6, 1053–1076.

Ratschbacher L., Frisch W., Linzer H.G., Sperner B., Meschede M., Decker K., Nemčok M., Nemčok J. & Grygar J. 1993: The Pieniny Klippen Belt in the Western Carpathians of north eastern Slovakia: structural evidence for transpression. *Tectonophysics* 226, 1–4, 471–483.

Rebesco M., Della Vedova B., Cernobori L. & Aloisi G. 2000: Acoustic facies of Holocene megaturbidites in the Eastern Mediterranean. *Sed. Geol.* 135, 65–74.

Reeder M.S., Rothwell R.G. & Stow D.A.V. 2000: Influence of sea level and basin physiography on emplacement of the late Pleistocene Herodotus Basin Megaturbidite (HBM), SE Mediterranean Sea. *Mar. Petrol. Geol.* 17, 199–218.

Remacha E. & Fernández L.P. 2003: High-resolution correlation patterns in the turbidite systems of the Hecho Group (South-Central Pyrenees, Spain). *Mar. Petrol. Geol.* 20, 711–726.

Ricci Lucchi F. 1990: Turbidites in foreland and on-thrust basin of the northern Apennines. *Palaeogeogr. Palaeoclimatol. Palaeoecol.* 77, 51–66.

Ricci Lucchi F. & Valmori E. 1980: Basin-wide turbidites in a Miocene, oversupplied deep-sea plain: a geometrical analysis. *Sedimentology* 27, 241–270.

Robin G. de Q. 1988: The Antarctic ice sheet, its history and respondence to sea level and climatic changes over the past 100 million years. *Palaeogeogr. Palaeoclimatol. Palaeoecol.* 67, 31-50.

Rodríguez-Pascua M.A., Calvo J.P., De Vicente G. & Gómez-Gras D. 2000: Soft-sediment deformation structures interpreted as seismites in lacustrine sediments of the Prebetic Zone, SE Spain, and their potential use as indicators of earthquake magnitudes during the Late Miocene. *Sed. Geol.* 135, 117–135.

Rossetti D.F. 1999: Soft-sediment deformation structures in late Albian to Cenomanian deposits, Sao Luis Basin, northern Brazil: evidence for palaeoseismicity. *Sedimentology* 46, 1065–1081.

Rothwell R.G., Reeder M.S., Anastasakis G., Stow D.A.V., Thomson J. & Kähler G. 2000: Low sea-level stand emplacement of megaturbidites in the western and eastern Mediterranean Sea. *Sed. Geol.* 135, 75–88.

Samuel O. & Fusán O. 1992: Reconstruction of subsidence and sedimentation of Central Carpathian Paleogene. *Západ. Karpaty, Sér. Geol.* 16, 7–46.

Sérguret M., Labaume P. & Madariaga R. 1984: Eocene seismicity in the Pyrenees from megaturbidites in the South-Pyrenean basin (North Spain). *Mar. Geol.* 55, 117–131.

Shanmugam G. & Moiola R.J. 1982: Eustatic control of turbidite deposition and winnowed turbidites. *Geology* 10, 231–235.

Sliva Ľ. 2005: Sedimentary facies of the Central Carpathians Paleogene Basin in the Spišská Magura Mts. *PhD Thesis*, Bratislava, 1–137.

Soták J. 1998: Sequence stratigraphy approach to the Central Carpathian Paleogene (Eastern Slovakia): eustasy and tectonics as controls of deep-sea fan deposition. *Slovak Geol. Mag.* 4, 185–190.

Soták J. 2010: Paleoenvironmental changes across the Eocene-Oligocene boundary: insights from the Central-Carpathian Paleogene Basin. *Geol. Carpathica* 61, 5, 1–26.

Soták J. & Starek D. 1999: Depositional stacking of the Central-Carpathian Paleogene Basin: sequences and cycles. *Geol. Carpathica* 50, 69–72.

Soták J., Pereszlenyi M., Marschalko R., Milička J. & Starek D. 2001: Sedimentology and hydrocarbon habitat of the submarine-fan deposits of the Central Carpathian Paleogene Basin (NE Slovakia). *Mar. Petrol. Geol.* 18, 87–114.

Soták J., Gedl P., Banská M. & Starek D. 2007: New stratigraphic data from the Paleogene formations of the Central Western Carpathians at the Orava region: Results of integrated micropaleontological study in the Pucov section. *Miner. Slovaca* 39, 89–106.

Spezzaferri S. 1994: Planktonic foraminiferal biostratigraphy and taxonomy of the Oligocene and lower Miocene in the oceanic record: an overview. *Palaeontogr. Ital.* 81, 1–187, tavv- 1–19.

Starek D. 2001: Sedimentology and paleodynamics of the Paleogene formations of the Central Western Carpathians in the Orava region. [Sedimentológia a paleodynamika paleogénnych formácií Centrálnych Západných Karpát na Orave.] *PhD Thesis*, *Geol. Inst. SAS*, Bratislava, 1–152 (in Slovak).

Starek D., Andreyeva-Grigorovich A.S. & Soták J. 2000: Suprafan deposits of the Biely Potok Formation in the Orava region: Sedimentary facies and nannoplankton distribution. *Slovak Geol. Mag.* 6, 2–3, 188–190.

Starek D., Sliva Ľ. & Vojtko R. 2004: The channel-levee sedimentary facies and their synsedimentary deformation: a case study from Huty Formation of the Podtatranská skupina Group (Western Carpathians). *Slovak Geol. Mag.* 10, 3, 177–182.

Starek D., Sliva Ľ. & Vojtko R. 2012: Eustatic and tectonic control on late Eocene fan delta development (Orava Basin, Central Western Carpathians). *Geol. Quart.* 56, 1, 67–84.

Švábenická L., Bubík M. & Stráník Z. 2007: Biostratigraphy and paleoenvironmental changes on the transition from the Menilite to Krosno lithofacies (Western Carpathians, Czech Republic). *Geol. Carpathica* 58, 3, 237–262.

Talling P.J., Amy L.A. & Wynn R.B. 2007: New insight into the evolution of large-volume turbidity currents: comparison of turbidite shape and previous modelling results. *Sedimentology* 54, 737–769.

Tinterri R., Drago M., Consonni A., Davoli G. & Mutti E. 2003: Modeling subaqueous bipartite sediment gravity flows on the basis of outcrop constrains: first results. *Mar. Petrol. Geol.* 20, 911–933.

Tripsanas E., Piper D.J.W., Jenner K.A. & Bryant W.R. 2008: Sedimentary characteristics of submarine mass-transport deposits: New perspectives from a corebased facies classification. *Sedimentology* 55, 97–136.

Vail P.R., Mitchum R.M. Jr. & Thompson III., S. 1977: Seismic

stratigraphy and global changes in sea-level. Part 3: Relative changes of sea level from coastal onlap. In: Payton C.E. (Ed.): Seismic stratigraphy — Application to hydrocarbon exploration. *Mem. Amer. Assoc. Petrol. Geol.* 26, 63–81.

Van Den Berg J.H., Van Gelder A. & Mastbergen D.R. 2002: The importance of breaching as a mechanism of subaqueous slope failure in fine sand. *Sedimentology* 49, 81–95.

Yose L.A. & Haller P.L. 1989: Sea-level control of mixed–carbonate-siliciclastic, gravity-flow deposition: Lower part of Keeler Canyon Formation (Pennsylvanian), southeastern California. *Geol. Soc. Amer. Bull.* 101, 427–439.

Zachos J.C., Lohmann K.C., Walker J.C.G. & Wise S.W. 1993: Abrupt climate change and transient climates during the Paleogene: a marine perspective. *J. Geol.* 101, 191–223.